

**THERMODYNAMIC MODELING AND OPTIMIZATION OF A  
SCREW COMPRESSOR CHILLER AND COOLING TOWER  
SYSTEM**

A Thesis

by

RHETT DAVID GRAVES

Submitted to the Office of Graduate Studies of  
Texas A&M University  
in partial fulfillment of the requirements for the degree of  
MASTER OF SCIENCE

December 2003

Major Subject: Mechanical Engineering

**THERMODYNAMIC MODELING AND OPTIMIZATION OF A  
SCREW COMPRESSOR CHILLER AND COOLING TOWER  
SYSTEM**

A Thesis

by

RHETT DAVID GRAVES

Submitted to Texas A&M University  
in partial fulfillment of the requirements  
for the degree of

MASTER OF SCIENCE

Approved as to style and content by:

---

Charles H. Culp  
(Co-Chair of Committee)

---

Warren M. Heffington  
(Co-Chair of Committee)

---

Calvin B. Parnell, Jr.  
(Member)

---

Dennis L. O'Neal  
(Head of Department)

December 2003

Major Subject: Mechanical Engineering

## ABSTRACT

Thermodynamic Modeling and Optimization of a Screw Compressor Chiller and  
Cooling Tower System. (December 2003)

Rhett David Graves, B.S., Mississippi State University

Co-Chairs of Advisory Committee: Dr. Charles H. Culp  
Dr. Warren M. Heffington

This thesis presents a thermodynamic model for a screw chiller and cooling tower system for the purpose of developing an optimized control algorithm for the chiller plant. The thermodynamic chiller model is drawn from the thermodynamic models developed by Gordon and Ng (1996). However, the entropy production in the compressor is empirically related to the pressure difference measured across the compressor. The thermodynamic cooling tower model is the Baker & Shryock cooling tower model that is presented in *ASHRAE Handbook – HVAC Systems and Equipment* (1992). The models are coupled to form a chiller plant model which can be used to determine the optimal performance. Two correlations are then required to optimize the system: a wet-bulb/setpoint correlation and a fan speed/pump speed correlation. Using these correlations, a “quasi-optimal” operation can be achieved which will save 17% of the energy consumed by the chiller plant.

## **DEDICATION**

Soli Deo Gloria.

## TABLE OF CONTENTS

ABSTRACT .....	iii
DEDICATION .....	iv
TABLE OF CONTENTS .....	v
LIST OF FIGURES .....	vi
LIST OF TABLES .....	viii
INTRODUCTION .....	1
LITERATURE REVIEW OF CHILLER & COOLING TOWER MODELS .....	5
APPLICATION .....	9
CHILLER MODEL DEVELOPMENT .....	15
COOLING TOWER MODEL DEVELOPMENT .....	31
COUPLING THE MODELS .....	39
OPTIMIZATION STRATEGY AND ANALYSIS .....	47
CONCLUSIONS .....	54
REFERENCES .....	56
APPENDIX A. COMPLETE CHILLER DERIVATION .....	59
APPENDIX B. TEMPERATURE-ENTROPY DIAGRAM EXPLANATION .....	88
VITA .....	97

## LIST OF FIGURES

FIGURE	Page
Figure 1.1. 205-ton Installed Screw Chiller.....	2
Figure 3.1. Test Facility .....	10
Figure 3.2. First-Floor Layout of the Test Facility .....	10
Figure 3.3. Second-Floor Layout of the Test Facility.....	11
Figure 3.4. Building Automation System Diagram .....	13
Figure 4.1. Chiller Energy Balance Diagram .....	17
Figure 4.2. Measured Power vs. Calculated Power (Gordon-Ng Model) .....	20
Figure 4.3. Measured Power vs. Calculated Power (Derived Evaporator Model) .....	22
Figure 4.5. Change in Pressure vs. Change in Coolant Leaving Temperatures .....	28
Figure 4.6. Change in Refrigerant Temperature vs. Change in Pressure .....	28
Figure 4.7. Chiller Model Flow Chart .....	30
Figure 5.1. Test Facility Cooling Tower.....	31
Figure 5.2. Cooling Tower Diagram.....	36
Figure 5.3. Condenser Water Entering Temperature Comparison .....	38
Figure 6.1. Chiller Plant Power Comparison (without offsets) .....	41
Figure 6.2. Chiller Plant Power Comparison (with offsets) .....	42
Figure 6.3. Condenser Water Entering Temperature Error .....	43
Figure 6.4. Condenser Water Leaving Temperature Error .....	44
Figure 6.5. Condenser Refrigerant Temperature Error.....	44

FIGURE	Page
Figure 6.6. Condenser Refrigerant Pressure Error.....	45
Figure 6.7. Compressor Power Error .....	45
Figure 7.1. Optimized Chiller Plant Power Comparison .....	48
Figure 7.2. Typical Cooling Tower Fan VFD Control Loop.....	49
Figure 7.3. Cooling Tower Setpoint vs. Wet-Bulb Temperature .....	50
Figure 7.4. Condenser Water Pump Speed vs. Cooling Tower Fan Speed .....	51
Figure 7.5. Quasi-Optimal Control Loop.....	52
Figure 7.6. Quasi-Optimal Chiller Plant Power Comparison .....	53

**LIST OF TABLES**

TABLE	Page
Table 5.1. Cooling Tower Node Values .....	37
Table 6.1. Inputs and Outputs of Chiller-Tower Model .....	39
Table 6.2. Output Offsets .....	41
Table 6.3. Standard Deviations for Each Component .....	46



## INTRODUCTION

The performance of the air conditioning system in most facilities can be improved by 10% to 30% (Braun 1988, Weber 1988). Large industrial and commercial facilities often employ a chilled water system to provide cooling to the space. These systems typically consist of air handling units, chillers and cooling towers. Figure 1.1 shows the 205-ton screw chiller installed in the test facility.

In order to effectively evaluate and improve the performance of these devices, a thermodynamic model of each component has been developed to analyze changes in energy consumption with respect to changes in control variables. As such models have developed over time, certain variables have been treated as constant in order to simplify the mathematical complexity. This is certainly true of modeling chilled-water and condenser-water flow rates. Few chiller plants modulate the chilled-water and condenser-water flow rates, and so, the assumption of constant values for these parameters is valid for the modeling of a chiller (Hartman 2001). This approach also allows the modeling of air-conditioning systems by treating each component individually. However, to calculate the lowest possible energy consumption for the system, the coupling between the chiller and the cooling tower, including the power consumption by the chilled-water and condenser-water pumps must be considered.

---

This thesis follows the style and format of the *International Journal of Heating, Ventilating, Air-Conditioning and Refrigerating Research*.

Reducing the chilled-water flow rate has energy-reduction advantages in variable-air-volume systems, but these advantages are limited for a constant-volume system (Cascia 2000). Cooling coils are designed to cool the air in the space and to provide humidity removal.



Figure 1.1. 205-ton Installed Screw Chiller

Reducing the chilled-water flow in a constant-volume system will raise the average temperature leaving the cooling coil, thus reducing the amount of latent heat

removed from the air. For this reason, the chilled-water flow rate is typically not varied in a chiller plant.

On the other hand, reducing the condenser-water flow rate has two advantages. The first advantage is the obvious reduction in pumping power associated with moving the condenser water between the cooling tower and chiller. The second advantage is an increase in cooling tower effectiveness. As the condenser-water flow rate is decreased, the temperature of the water entering the tower is increased. This elevated water temperature provides the tower with a greater enthalpy difference between the entering air and water streams, which means there is more driving potential for heat transfer in the cooling tower (Kirsner 1996). As the condenser-water flow rate is reduced, the compressor power will increase due to the elevation in average condenser temperature. However, there is an optimal operating point where the sum of the compressor power, the condenser-water pumping power, and the cooling tower fan power is a minimum. Simply modeling the components in a chilled water system will not reveal the savings in pumping power unless the chiller and cooling tower models are coupled with varying condenser water flow rate.

In Section 2, a literature review of chiller models, cooling tower models, and combinations of these models will be presented. The particular modeling application will be described in Section 3. This work will develop a thermodynamically coupled model of a chiller and cooling tower including variable condenser-water flow rate in Sections 4 and 5, respectively. Section 6 will discuss the coupling of the chiller and cooling tower model. The model allows optimization of the system by minimizing

power consumption. It was validated using measured data from a commercial building installation. The model can then be used to predict the behavior of the chiller plant under a variety of conditions, which then will be used to implement control algorithms for the chiller plant as discussed in Section 7.

## **LITERATURE REVIEW OF CHILLER & COOLING TOWER MODELS**

A literature search revealed that much work has been done in the area of chiller plant component modeling, but it did not yield a satisfactory model of coupled chillers and cooling towers. Most cross-flow cooling tower models employ a nodal analysis that looks at the change in tower water temperature versus the change in air enthalpy across the tower fill (ASHRAE Handbook 1992, Weber 1988). This particular model assumes that there is no water loss due to evaporation. An improvement to include the water loss due to evaporation shows that there is only a 1% to 3% change in cooling tower water flow if the evaporation is considered (Braun 1988). Another popular cooling tower model was developed at the Environmental Engineering Laboratory of the Chamber of Mines of South Africa (Whillier 1976). This model introduces a tower capacity factor that is used to predict tower performance. Also presented is the idea that there is an optimal water flow rate for a given set of outside conditions to minimize the average water temperature across the cooling tower.

Thermodynamic models of reciprocating chillers (Chua et al. 1996) and centrifugal chillers (Gordon et al. 1995) have been developed, but a thermodynamic model of a screw chiller was not found. However, a universal thermodynamic model for chillers is available with fundamental characteristics that apply to all chiller models: vapor compression, absorption, thermoelectric, and thermoacoustic (Gordon and Ng 1995). Chiller models have been used to predict the performance of thermal storage

systems (Henze et al. 1997) and whole chiller plant systems (Lau et al. 1985). Chiller models have also been used to aid in the development of control algorithms for chiller plants (Flake et al. 1997).

There have been several attempts to generate an “optimal” operating scheme using the Whillier cooling tower model, a chiller model, or a combination of both. Many authors present “optimized” operation by considering the speed of the compressor, particularly in centrifugal and screw compressors (Braun 1988, Rolfsman and Wihlborg 1996, Gordon and Ng 2000, Hartman 2001). Within a screw compressor, there are two methods for controlling the mass flow rate of refrigerant through the compressor. One controls compressor speed and the second uses a “slider”, essentially a gate valve on top of the compressor compartment, to control the flow of refrigerant. An “optimized” screw chiller control strategy using the “slider” is presented by Hitachi (Aoyama and Izushi 1990). Further chiller optimization compares multiple-input, multiple-output (MIMO) and single-input, single-output (SISO) control of the compressor speed and expansion valve settings (He et al. 1998). Multiple-chiller plants can be optimized by ensuring that each chiller is operating near its own optimal point (Austin 1991).

An “optimized” control of a cooling tower has been developed utilizing condenser water flow rate and cooling tower fan speed as the control variables (Van Dijk 1985). The idea that the average water temperature determines the capacity of the tower was used to suggest that, during a retrofit, a cooling tower’s capacity may be increased by increasing the average water temperature (Schwedler and Bradley 2001). Another strategy for “optimized” control utilizes a fixed-approach tower setpoint (Burger 1993).

Another study showed that the fixed-approach tower setpoint method of optimization was not as effective as an optimization technique based on tower range (Stout and Leach 2002). Although these control strategies do optimize the operation of one component, they do not optimize the system.

Trane engineers have shown that reducing cooling tower fan power, although that action may increase chiller compressor power, actually results in a lower overall power consumption operating point (Schwedler 1998). This work was a natural extension of the idea that controlling cooling tower leaving temperature setpoint and compressor power would provide “near optimal” control of a chiller plant (Braun and Diederich 1990). In an effort to control electrical demand, thermal storage systems have been designed to take advantage of the relationship between chiller power and electrical rate structures (Henze et al. 1997). Controlling the condenser water flow rate has been discussed (Lau et al. 1985), but a useful thermodynamic model has not been published. The effect of controlling the chilled water side of operations has been investigated as well (Cascia 2000). These efforts were attempts to optimize the system rather than individual components, but none of these included the three components compressor power, cooling tower fan power, and condenser water pumping power.

Artificial neural networks have been used with building automation systems to optimize the performance of a system (Gibson 1997), however, this optimization technique is very complicated to understand and employ. With the exception of the papers mentioning condenser water flow rate as a control variable for reducing the power consumption of the entire chiller plant (Lau et al. 1985) and the effect of varying

the condenser water flow rate on the chiller (Gordon 2000), little has been done to explain the relationship between compressor power, cooling tower fan power and condenser water pumping power. Currently a single model that represents all three components does not exist in the published literature.



## APPLICATION

The test facility for this thesis is an office and laboratory building located on the campus of a defense contractor in Fort Worth, Texas. The building is a two-story building of brick construction with windows in the perimeter walls. The approximate window area is 2,888 square feet. The exterior wall area, not including the window area, is 13,112 square feet. The roof is of modified bitumen construction and covers an area of 35,553 square feet. The first-floor conditioned floor space is 30,400 square feet, while the second-floor conditioned floor space is 25,600 square feet. Figure 3.1 shows a picture of the test facility. Figures 3.2 and 3.3 show the first- and second-floor layouts of the building, respectively. The crosshatched area is the unconditioned mechanical room.



Figure 3.1. Test Facility

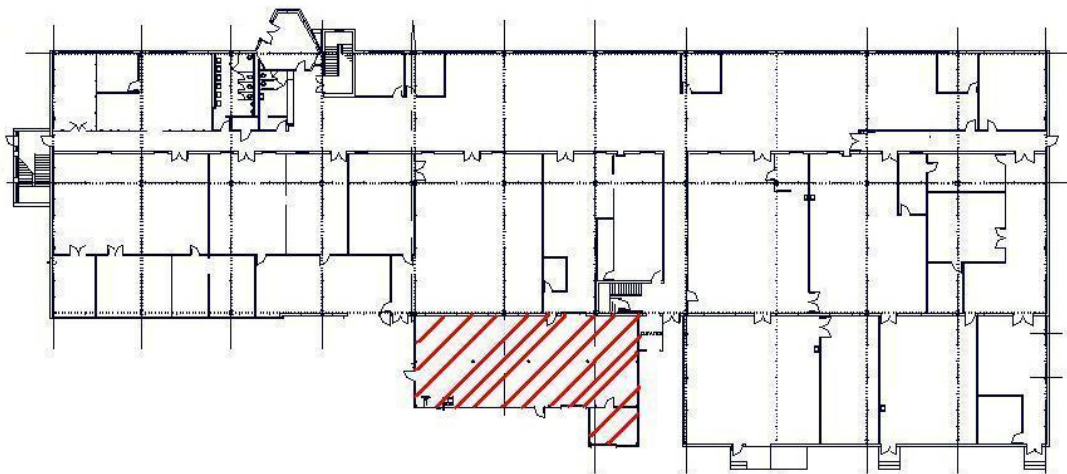


Figure 3.2. First-Floor Layout of the Test Facility

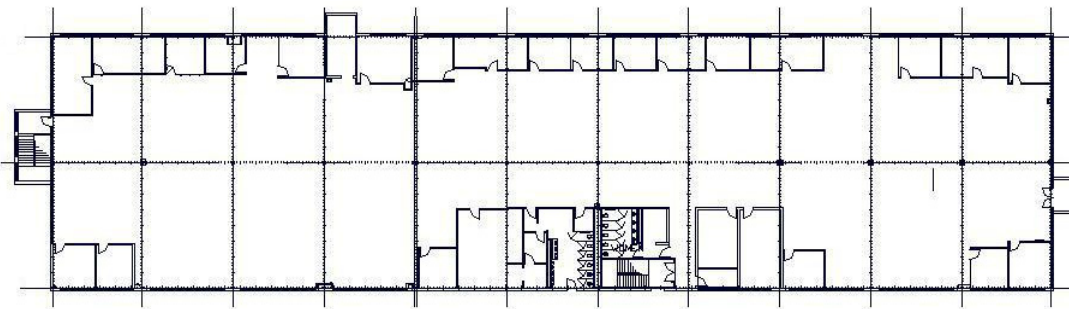


Figure 3.3. Second-Floor Layout of the Test Facility

The air conditioning load on the first floor of the building is divided into two distinct types of areas: office and lab. The load in the office area is attributed to lighting, computers, people and solar heat gain through the exterior walls and windows. The lab area is located on the south side of the building in a single story building addition with approximately 10-ft. high ceilings. The load in the lab area is attributed to two autoclaves, hydraulic pumping equipment, lighting, computers, people and solar heat gain through the exterior walls and roof. The second floor of the building is office space. The load in this area is attributed to lighting, computers, people and solar heat gain through the exterior walls, windows and roof. The building is occupied between the hours of 6 a.m. and 6 p.m. during weekdays.

There are seven air-handling units that serve the building. There are four large multi-zone air-handling units that serve the large office areas and three small single-zone air-handling units that control the lab areas of the building. These air-handling units feature blow-through coils with the heating coil located upstream of the cooling coil.

There are a number of fan-coil cooling units for individual offices throughout the building. The chiller plant in this building also provides chilled water for two air-handling units in the cafeteria of an adjoining building and the fan-coil units for the office area of an adjacent building.

The chiller plant includes two identical 205-ton helical rotary screw chillers, Trane model RTHC-B2C2D2 of the type shown in Figure 1.1. The chillers are designed to produce 43 °F water with a chilled water return temperature of 53 °F and a condenser entering water temperature of 85 °F. The chiller plant is designed to operate in a primary-secondary format so that the second chiller will only operate when the chilled water temperature exceeds 47 °F.

A 400-ton cooling tower cools the condenser water for both chillers. The cooling tower fan is powered by a 25-hp motor that is equipped with a variable-speed drive. The variable-speed drive works to maintain a tower leaving set point, when attainable. Currently the cooling tower set point is 80 °F.

Two 20-hp, 600-gpm condenser water pumps circulate water between the cooling tower and chillers. Each condenser pump is assigned to a particular chiller so that the pump only operates when its designated chiller operates. Two 25-hp, 410-gpm chilled water pumps circulate water between the chillers and the air-handling units. Like the condenser pumps, each chilled water pump is assigned to a particular chiller.

A proprietary automated building software program controls the building. This control system consists of programmable control modules (PCMs), building control units (BCUs), and an operator-interface workstation as shown in Figure 3.4.

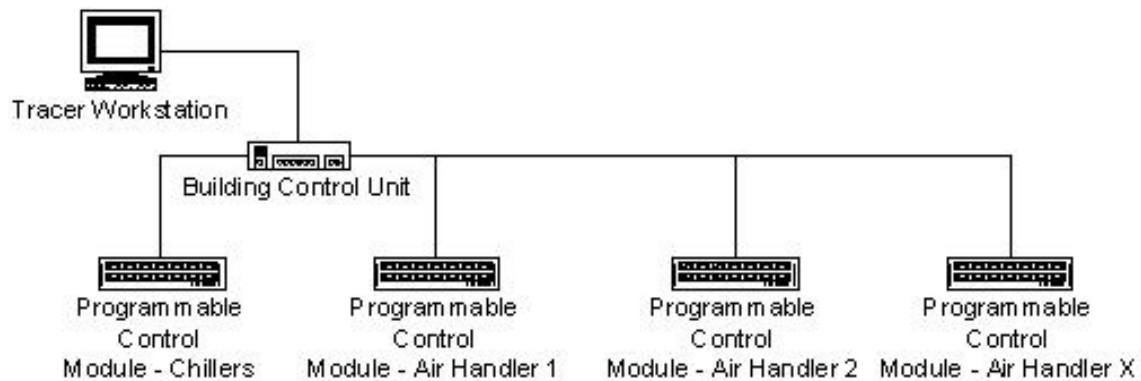


Figure 3.4. Building Automation System Diagram

System measurements are made with devices that are connected to the PCMs. The PCM is capable of receiving 4-20mA signals. The conversion of this signal to a digital value takes place in the PCM. Time-keeping and the trending of data takes place in the BCU. The BCU is only capable of trending data with a resolution of 1 minute (Stagg 2003). A scheduled data trend is initiated by an operator using the interface software and then uploaded to the BCU. The data trend will then run continuously and replace data on a first-in-first-out basis. The BCU is capable of storing 244 samples per trend. The number of trends that the BCU is capable of recording is limited by the memory card space available in the BCU. The time is applied to the trend when the data is requested by the BCU. The time between the trend request and the actual time that the data is recorded is separated by the scan rate between the BCU and PCM (Stagg 2003). The BCU periodically scans each PCM for every input in the PCM. The scan rate is dependent upon the load on the communications system. The BCU will scan a fully-loaded system every 63 seconds. At the current communications loading, the BCU will

scan the PCMs for new data every 18 seconds. This means that a trend that is scheduled to record every minute will have data that is no older than 18 seconds. For the purpose of generating a steady-state model, the data acquisition capabilities of this system are adequate.

In order to obtain the data, the operator must initiate the reporting feature. The report is stored in the BCU and collects the specified trends into one document, which is uploaded to the operator-interface workstation. Each upload takes place on a schedule specified by the operator. The uploaded data is then added to a data file that is stored on the workstation. The data storage on the workstation is limited by the hard-drive space available on the workstation.

## CHILLER MODEL DEVELOPMENT

The First Law equation that describes the refrigerant-side operation of a chiller is

$$\Delta E = 0 = Q_{\text{cond}} + Q_{\text{cond}}^{\text{leak}} - Q_{\text{evap}} - Q_{\text{evap}}^{\text{leak}} - P_{\text{in}} + Q_{\text{comp}}^{\text{leak}} \quad (4.1)$$

where

$Q_{\text{cond}}$  = heat transfer in the condenser (refrigerant to water), kW,

$Q_{\text{cond}}^{\text{leak}}$  = heat transfer from the condenser piping to the environment, kW,

$Q_{\text{evap}}$  = heat transfer in the evaporator (water to refrigerant) , kW,

$Q_{\text{evap}}^{\text{leak}}$  = heat transfer from the evaporator piping to the environment, kW,

$P_{\text{in}}$  = compressor power input, kW,

$Q_{\text{comp}}^{\text{leak}}$  = heat transfer from the compressor to the environment, kW.

The Second Law equation is

$$\Delta S = 0 = \left( \frac{Q_{\text{cond}} + Q_{\text{cond}}^{\text{leak}}}{T_{\text{cond}}^{\text{refr}}} \right) - \left( \frac{Q_{\text{evap}} + Q_{\text{evap}}^{\text{leak}}}{T_{\text{evap}}^{\text{refr}}} \right) - \Delta S_{\text{internal}} \quad (4.2)$$

where

$T_{\text{cond}}^{\text{refr}}$  = temperature of the condensing refrigerant, R,

$T_{\text{evap}}^{\text{refr}}$  = temperature of the evaporating refrigerant, R,

$\Delta S_{\text{internal}}$  = internal entropy production, kW/R.

Equations (4.1) and (4.2) are combined to give:

$$P_{\text{in}} = -Q_{\text{evap}} + \frac{Q_{\text{evap}} T_{\text{cond}}^{\text{refr}}}{T_{\text{evap}}^{\text{refr}}} + T_{\text{cond}}^{\text{refr}} \Delta S_{\text{internal}} + T_{\text{cond}}^{\text{refr}} \left[ \frac{Q_{\text{comp}}^{\text{leak}}}{T_{\text{cond}}^{\text{refr}}} + Q_{\text{evap}}^{\text{leak}} \left( \frac{1}{T_{\text{evap}}^{\text{refr}}} - \frac{1}{T_{\text{cond}}^{\text{refr}}} \right) \right] \quad (4.3)$$

A more detailed derivation of equation (4.3) is shown in Appendix A. A graphical representation of equation (4.3) is shown in Figure 4.1.



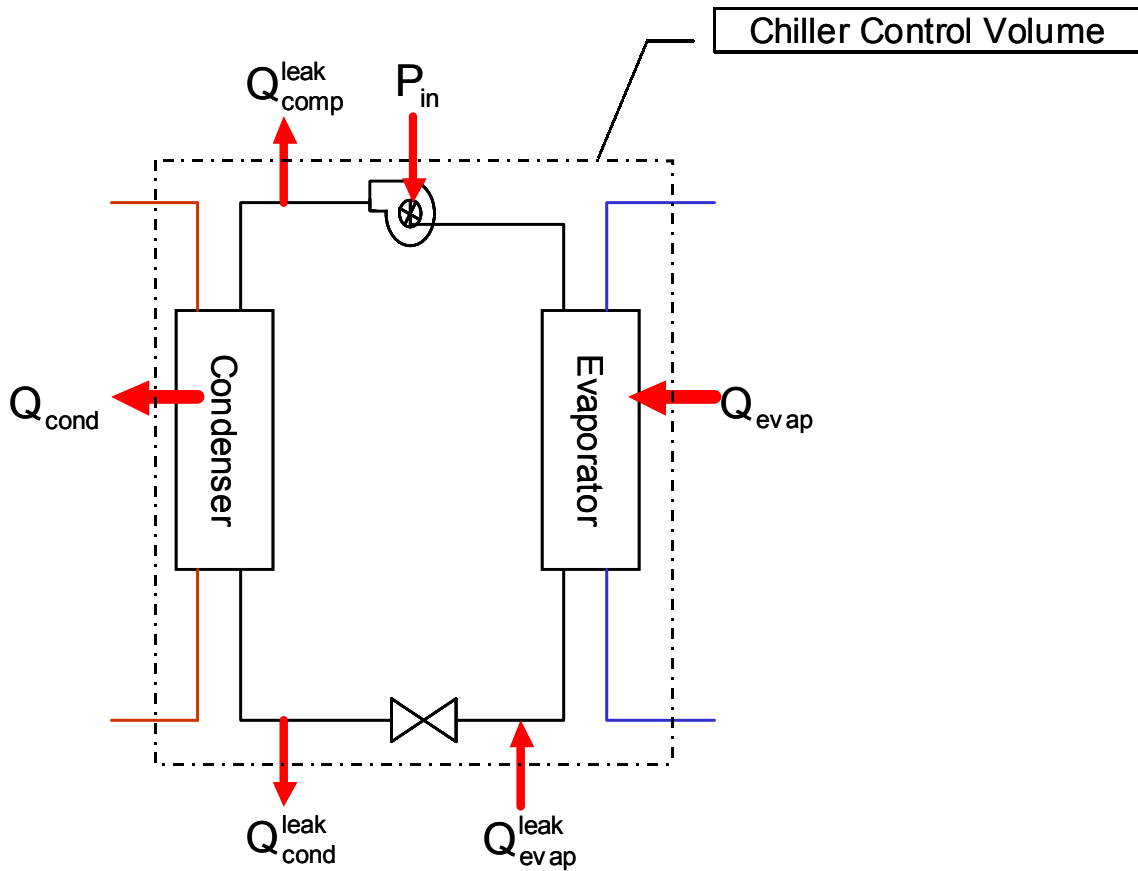


Figure 4.1. Chiller Energy Balance Diagram

The  $Q^{leak}$  terms in the brackets of equation (4.3) can then be described in terms of an entropy production term due to heat leaks. This entropy production term,  $\Delta S_{leak}$ , is defined to be:

$$\Delta S_{leak} \equiv \frac{Q_{comp}^{leak}}{T_{cond}^{refr}} + Q_{evap}^{leak} \left( \frac{1}{T_{evap}^{refr}} - \frac{1}{T_{cond}^{refr}} \right) \quad (4.4)$$

Inserting equation (4.4) into equation (4.3) gives a simplified thermodynamic equation that governs chiller performance:

$$P_{in} = -Q_{evap} + \frac{Q_{evap} T_{cond}^{refr}}{T_{evap}^{refr}} + T_{cond}^{refr} \Delta S_{internal} + T_{cond}^{refr} \Delta S_{leak} \quad (4.5)$$

$Q_{evap}$  can be expressed in terms of evaporator water inlet and outlet temperatures and the mass flow of water through the evaporator

$$Q_{evap} = (\dot{m}_w c_p)_{evap} (T_{evap}^{w\_in} - T_{evap}^{w\_out}) \quad (4.6)$$

where

$\dot{m}_w$  = coolant (water) mass flow rate, lb/min,

$c_p$  = coolant (water) specific heat, Btu/lb\*R,

$T_{evap}^{w\_out}$  = evaporator leaving water temperature, R,

$T_{evap}^{w\_in}$  = evaporator entering water temperature, R.

Inserting equation (4.6) into equation (4.5) gives

$$P_{in} = -(\dot{m}_w c_p)_{evap} (T_{evap}^{w\_in} - T_{evap}^{w\_out}) + \frac{(\dot{m}_w c_p)_{evap} (T_{evap}^{w\_in} - T_{evap}^{w\_out}) T_{cond}^{refr}}{T_{evap}^{refr}} + T_{cond}^{refr} \Delta S_{total} \quad (4.7)$$

where

$$\Delta S_{total} \equiv \Delta S_{internal} + \Delta S_{leak} \quad (4.8)$$

Equation (4.7) is an expression for  $P_{in}$  in terms of the chiller coolant temperatures, refrigerant temperatures, entropy changes, and the mass flow of coolant through the evaporator. Gordon and Ng claim that  $\Delta S_{total}$  is approximately constant for reciprocating and centrifugal chillers over a wide range of chiller loads (Gordon 2000). In order to calculate a constant  $\Delta S_{total}$ , the power, temperatures and mass flows were measured and equation (4.7) was solved for each set of values. The  $\Delta S_{total}$  terms for each individual point were averaged to arrive at a constant  $\Delta S_{total}$  term. Figure 4.2 shows the comparison of the calculated chiller power versus the measured chiller power if the assumption of a constant  $\Delta S_{total}$  is employed for the screw chiller. The data points represent the calculated power using equation (4.7) and the constant  $\Delta S_{total}$  term. Also shown is the ideal power line, where measured power equals calculated power. The use of a constant  $\Delta S_{total}$  term yields calculated values that are 4-5% lower than the ideal power line when the measured power is less than 45 kW. The calculated value varies

slightly ( $\pm 2\%$ ) from the ideal power line over the range of 45-55 kW. Above 55 kW, the calculated values are 10-12% higher than the ideal power line.

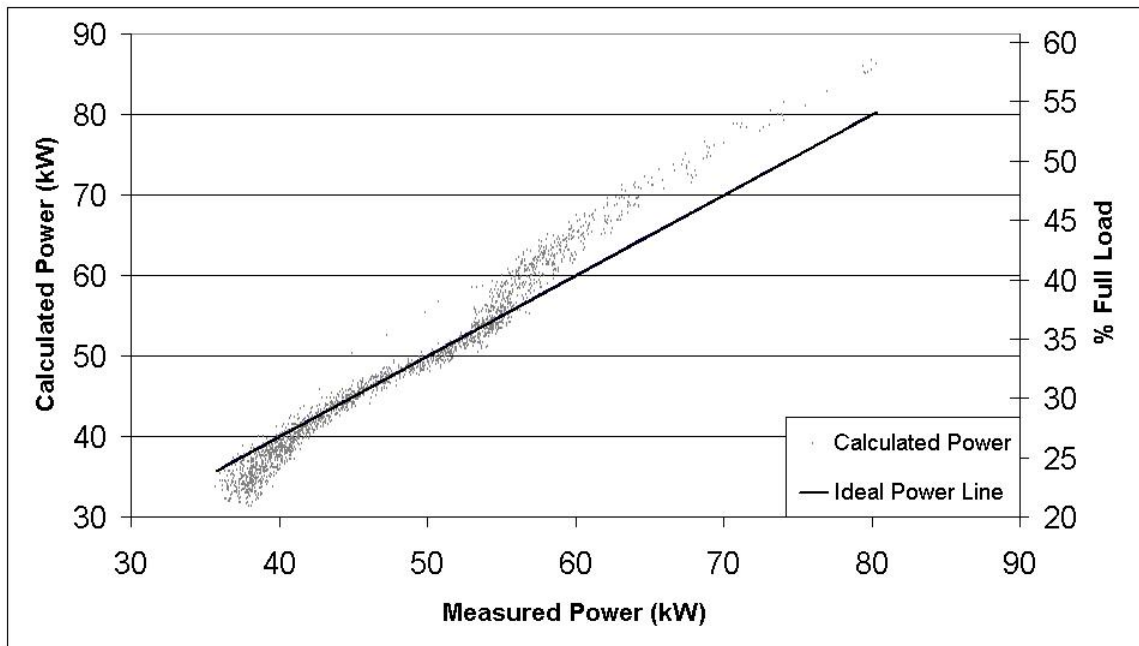


Figure 4.2. Measured Power vs. Calculated Power (Gordon-Ng Model)

For a screw compressor, the change in pressure across the compressor will impact the entropy change (Gordon and Ng 2000). Since the evaporation and condensation processes occur at constant pressures and temperatures, there is a strong correlation between the refrigerant condensation and evaporation temperatures and the refrigerant condensation and evaporation pressures, respectively. Consequently, there is a strong correlation between the change in pressure across the compressor and the difference between the condenser and evaporator refrigerant temperatures. Since the change in the log-mean temperature difference will change the effectiveness of the heat

exchanger, the difference in chilled water entering and leaving temperatures will also have an effect on  $\Delta S_{\text{total}}$ . These are the two physical mechanisms that will be considered in empirically determining an equation to describe  $\Delta S_{\text{total}}$ . An explanation of entropy production mechanisms from the Rankine Cycle diagram can be found in Appendix B. In order to account for these effects, equation (4.8) is solved for  $\Delta S_{\text{total}}$  and a multiple-linear regression for  $\Delta S_{\text{total}}$  as a function of chilled water temperature change and refrigerant temperature difference is performed. This line is described by:

$$\Delta S_{\text{total}} = -0.0001608(T_{\text{cond}}^{\text{refr}} - T_{\text{evap}}^{\text{refr}}) - 0.00176(T_{\text{evap}}^{\text{w\_in}} - T_{\text{evap}}^{\text{w\_out}}) + 0.05605 \quad (4.9)$$

Combining equations (4.7) and (4.9) yields an expression for  $P_{\text{in}}$  which allows the computation of chiller power using the evaporator coolant temperatures, refrigerant temperatures, and the mass flow of coolant through the evaporator. Figure 4.3 shows the power comparison using these variables and the temperature-entropy correlation for the evaporator side. The data points represent the calculated power using equations (4.7) and (4.9). The ideal power line again represents the series of points that would be obtained with a perfect chiller model. The use of the temperature-entropy correlation in equation (4.9) shows a calculated chiller power that are 3-5% higher than the ideal line for measured power values less than 48 kW. The calculated power is 2-3% lower than the measured power over the range of 48-55 kW. Above 55 kW, the calculated power is only 2-3% higher than the ideal line. The shape of the calculated power plot is due to

entropy effects that were not considered in this analysis. The effect of boiling and condensing refrigerant on the heat transfer in the evaporator and condenser is not considered. Also, the effect of the outside air conditions on the heat leaks to the environment is not considered. While these considerations would provide a more accurate chiller model, they only improve the model's accuracy by 2-3%. The added complexity is not necessary for the purpose of determining an algorithm to provide optimal chiller plant control.

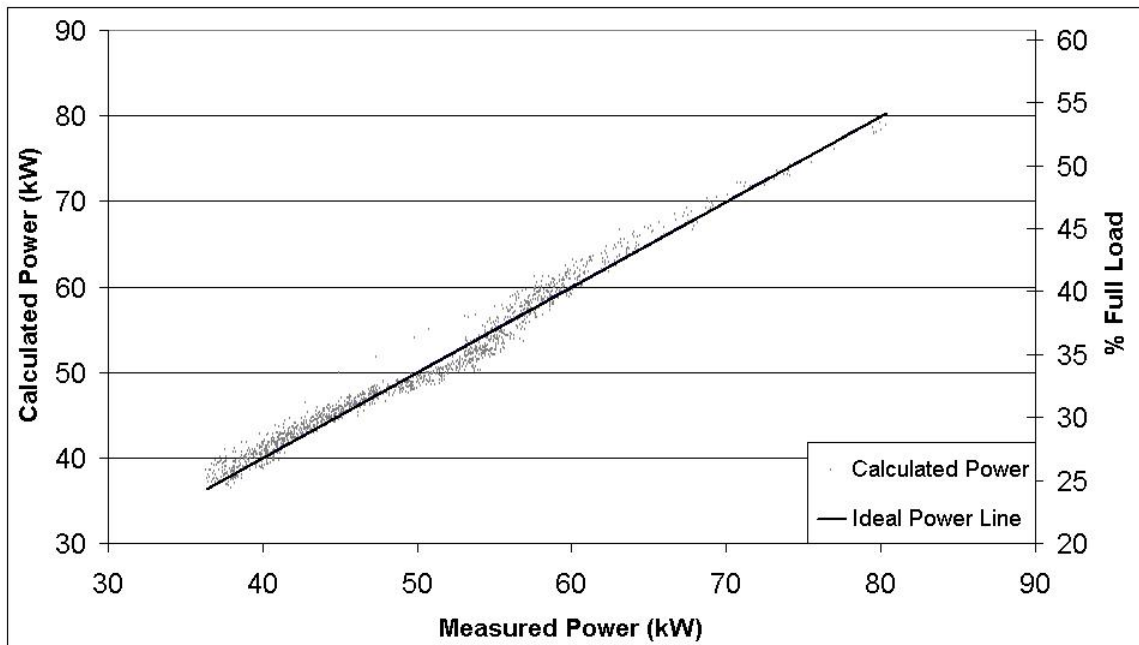


Figure 4.3. Measured Power vs. Calculated Power (Derived Evaporator Model)

In addition to the compressor power, the condenser pressure and condenser leaving water temperature are desired variables for calculation. The calculation of the

condenser pressure will ensure that the condenser pressures do not exceed the capability of the chiller. The calculation of the condenser leaving water temperature will be used in the cooling tower model to re-evaluate the condenser entering water temperature. In order to calculate these values, the chiller power input must be defined in terms of condenser variables. Previously, in equation (4.3), equations (4.1) and (4.2) were combined so that the  $Q_{\text{cond}}$  term would disappear. Equations (4.1) and (4.2) can also be combined to eliminate the  $Q_{\text{evap}}$  term. Combining equations (4.1) and (4.2) in this way yields:

$$P_{\text{in}} = Q_{\text{cond}} - \frac{Q_{\text{cond}} T_{\text{evap}}^{\text{refr}}}{T_{\text{cond}}^{\text{refr}}} + T_{\text{evap}}^{\text{refr}} \Delta S_{\text{internal}} + T_{\text{evap}}^{\text{refr}} \left[ \frac{Q_{\text{comp}}^{\text{leak}}}{T_{\text{evap}}^{\text{refr}}} + Q_{\text{cond}}^{\text{leak}} \left( \frac{1}{T_{\text{evap}}^{\text{refr}}} - \frac{1}{T_{\text{cond}}^{\text{refr}}} \right) \right] \quad (4.10)$$

The  $Q^{\text{leak}}$  terms in the brackets of equation (4.10) can then be described in terms of an entropy production term due to heat leaks. This entropy production term,  $\Delta S_{\text{leak}}$ , is defined to be:

$$\Delta S_{\text{leak}} \equiv \frac{Q_{\text{comp}}^{\text{leak}}}{T_{\text{evap}}^{\text{refr}}} + Q_{\text{cond}}^{\text{leak}} \left( \frac{1}{T_{\text{evap}}^{\text{refr}}} - \frac{1}{T_{\text{cond}}^{\text{refr}}} \right) \quad (4.11)$$

Inserting equation (4.11) into equation (4.10) gives:

$$P_{in} = Q_{cond} - \frac{T_{evap}^{refr} Q_{cond}}{T_{cond}^{refr}} + T_{evap}^{refr} \Delta S_{internal} + T_{evap}^{refr} \Delta S_{leak} \quad (4.12)$$

$Q_{cond}$  can be expressed as

$$Q_{cond} = (\dot{m}_w c_p)_{cond} (T_{cond}^{w\_out} - T_{cond}^{w\_in}) \quad (4.13)$$

where

$\dot{m}_w$  = coolant (water) mass flow rate through condenser, lb/min,

$c_p$  = coolant (water) specific heat, Btu/lb\*R,

$T_{cond}^{w\_out}$  = condenser leaving water temperature, R,

$T_{cond}^{w\_in}$  = condenser entering water temperature, R.

Inserting equation (4.13) into equation (4.12) gives

$$P_{in} = (\dot{m}_w c_p)_{cond} (T_{cond}^{w\_out} - T_{cond}^{w\_in}) - \frac{T_{evap}^{refr} (\dot{m}_w c_p)_{cond} (T_{cond}^{w\_out} - T_{cond}^{w\_in})}{T_{cond}^{refr}} + T_{evap}^{refr} \Delta S_{total} \quad (4.14)$$



where the  $\Delta S$  terms have again been combined using equation (4.8). As with the evaporator model, equation (4.15) is used to calculate  $\Delta S_{\text{total}}$  using the condenser measurements. A linear regression for  $\Delta S_{\text{total}}$  as a function of condenser water temperature change and refrigerant temperature difference is performed. This line is described by:

$$\Delta S_{\text{total}} = 0.0000666(T_{\text{cond}}^{\text{refr}} - T_{\text{evap}}^{\text{refr}}) - 0.00291(T_{\text{cond}}^{\text{w-out}} - T_{\text{cond}}^{\text{w-in}}) + 0.05132 \quad (4.15)$$

Combining equations (4.14) and (4.15) allows the computation of chiller power using the condenser coolant temperatures, refrigerant temperatures, and the mass flow of coolant through the condenser. Figure 4.4 shows the power comparison using these variables and the temperature-entropy correlation for the condenser side. The data points represent the calculated power using equations (4.14) and (4.15). Also shown is the ideal power line. The condenser model shows a calculated chiller power values that are within 5% of the values shown on the ideal chiller power line.

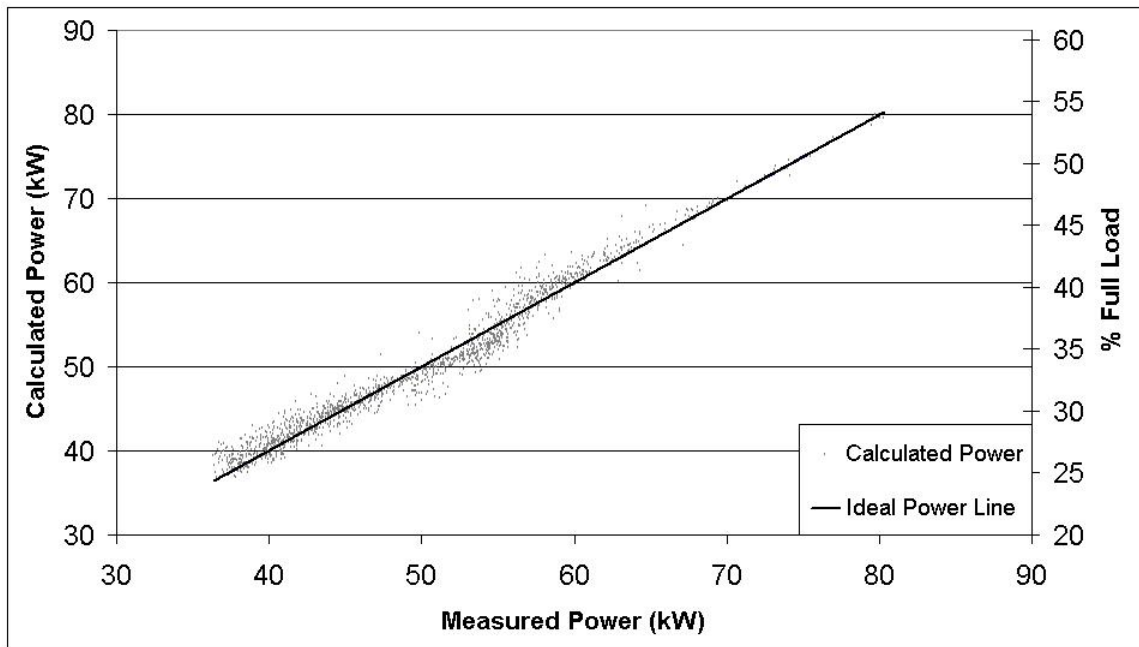


Figure 4.4. Measured Power vs. Calculated Power (Derived Condenser Model)

One of the desired outputs of this chiller model is the condenser leaving water temperature. The derived condenser model is used to predict the condenser leaving water temperature by rearranging the combination of equations (4.14) and (4.15). In order to calculate the condenser pressure, calculating the change in pressure across the compressor is necessary. As mentioned before, there is a strong correlation between the refrigerant condensation and evaporation temperatures and the refrigerant condensation and evaporation pressures, respectively. The leaving condenser and leaving evaporator coolant temperatures approach the condenser and evaporator refrigerant temperatures such that:

$$\Delta T_{\text{refr}} \approx T_{\text{cond}}^{\text{w-out}} - T_{\text{evap}}^{\text{w-out}} \quad (4.16)$$

Since  $\Delta T_{\text{refr}}$  is related to  $T_{\text{cond}}^{\text{w-out}} - T_{\text{evap}}^{\text{w-out}}$ , there is a relationship between  $T_{\text{cond}}^{\text{w-out}} - T_{\text{evap}}^{\text{w-out}}$  and  $\Delta P$ . This empirical relationship is shown in Figure 4.5. A linear regression of the data in Figure 4.5 provides the empirical correlation between the changes in refrigerant temperature and pressure. This line is described by:

$$\Delta P = 1.9464(T_{\text{cond}}^{\text{w-out}} - T_{\text{evap}}^{\text{w-out}}) - 20.946 \quad (4.17)$$

The change in pressure is then added to the measured evaporator pressure to calculate the pressure in the condenser of the chiller. The pressure in the condenser must be calculated since exceeding the chiller's maximum condenser pressure will cause a chiller failure. The empirical correlation between the change in refrigerant temperature and the change in pressure is shown in Figure 4.6. A linear regression of the data in Figure 4.6 gives:

$$\Delta T_{\text{refr}} = 0.5423(\Delta P) + 12.253 \quad (4.18)$$

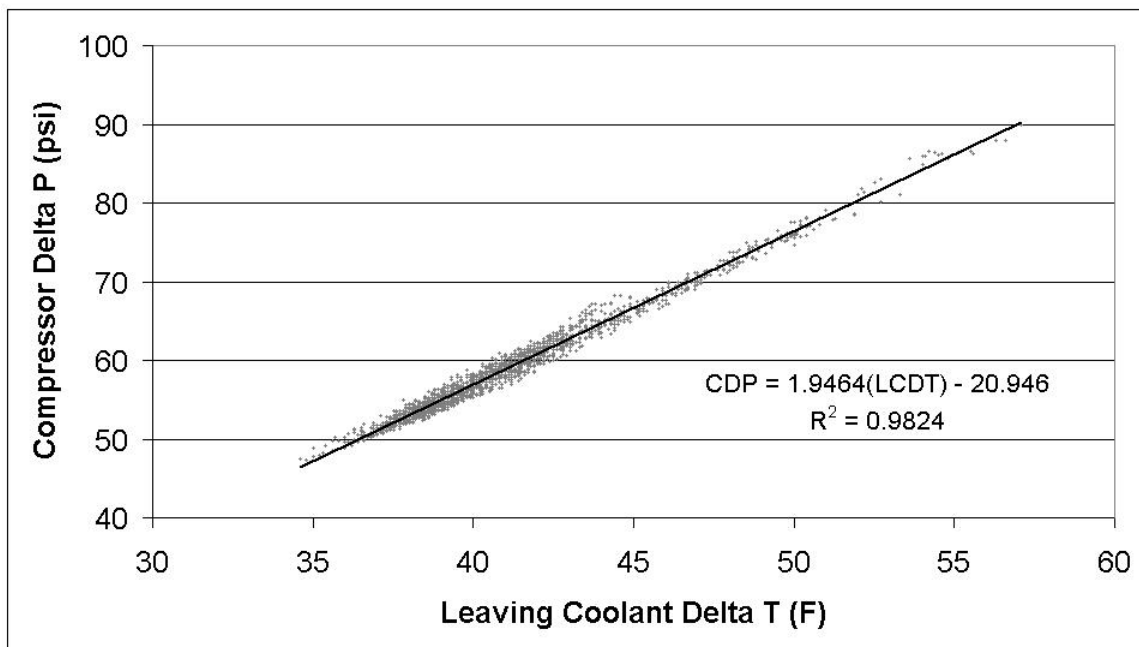


Figure 4.5. Change in Pressure vs. Change in Coolant Leaving Temperatures

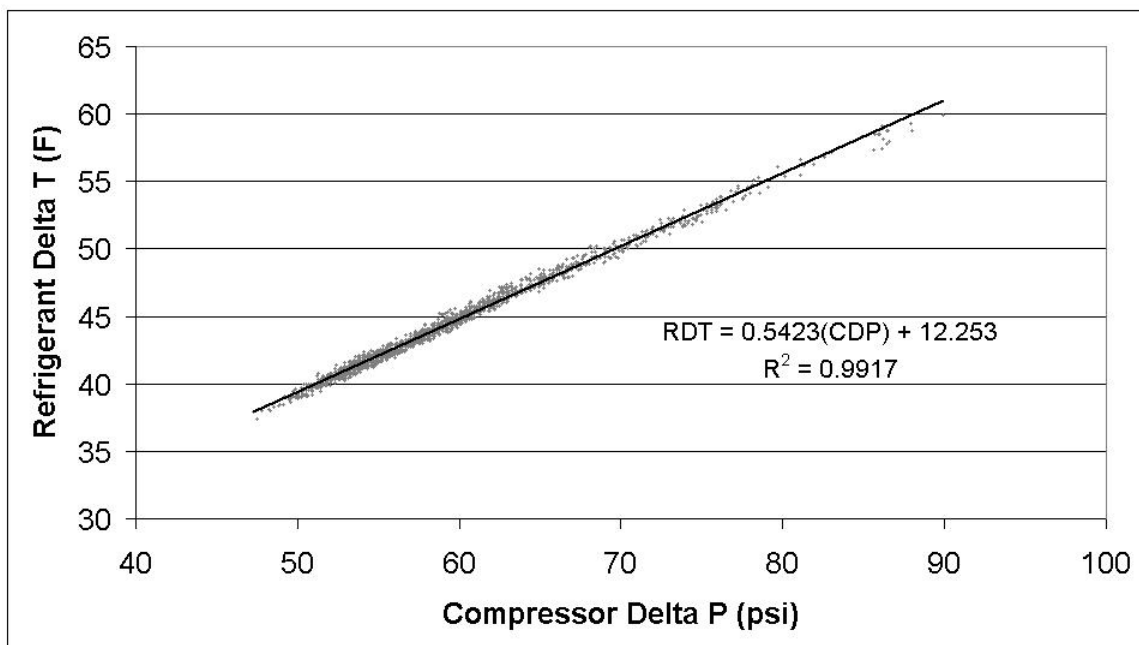


Figure 4.6. Change in Refrigerant Temperature vs. Change in Pressure

At this point an iterative solution is employed to calculate the chiller power consumption, the leaving condenser water temperature and the condenser pressure. Initial estimate values for the change in pressure across the compressor and the condenser refrigerant temperature are employed with measured evaporator temperatures and pressures to calculate the compressor power using equation (4.7). This compressor power is then used in equation (4.14) to calculate the condenser coolant leaving temperature. This temperature is used in equation (4.17) to calculate a new value for the change in pressure across the compressor. Equation (4.18) is employed to calculate the change in refrigerant temperatures. The condenser refrigerant temperature is given by:

$$T_{\text{cond}}^{\text{refr}} = T_{\text{evap}}^{\text{refr}} + \Delta T_{\text{refr}} \quad (4.19)$$

Equation (4.19) is used to calculate a new condenser refrigerant temperature. The new condenser refrigerant temperature and pressure is used in subsequent iterations. The model typically converges to 0.0025% with five iterations. A flow chart depicting the order of the chiller model calculations is shown in figure 4.7 on the following page.

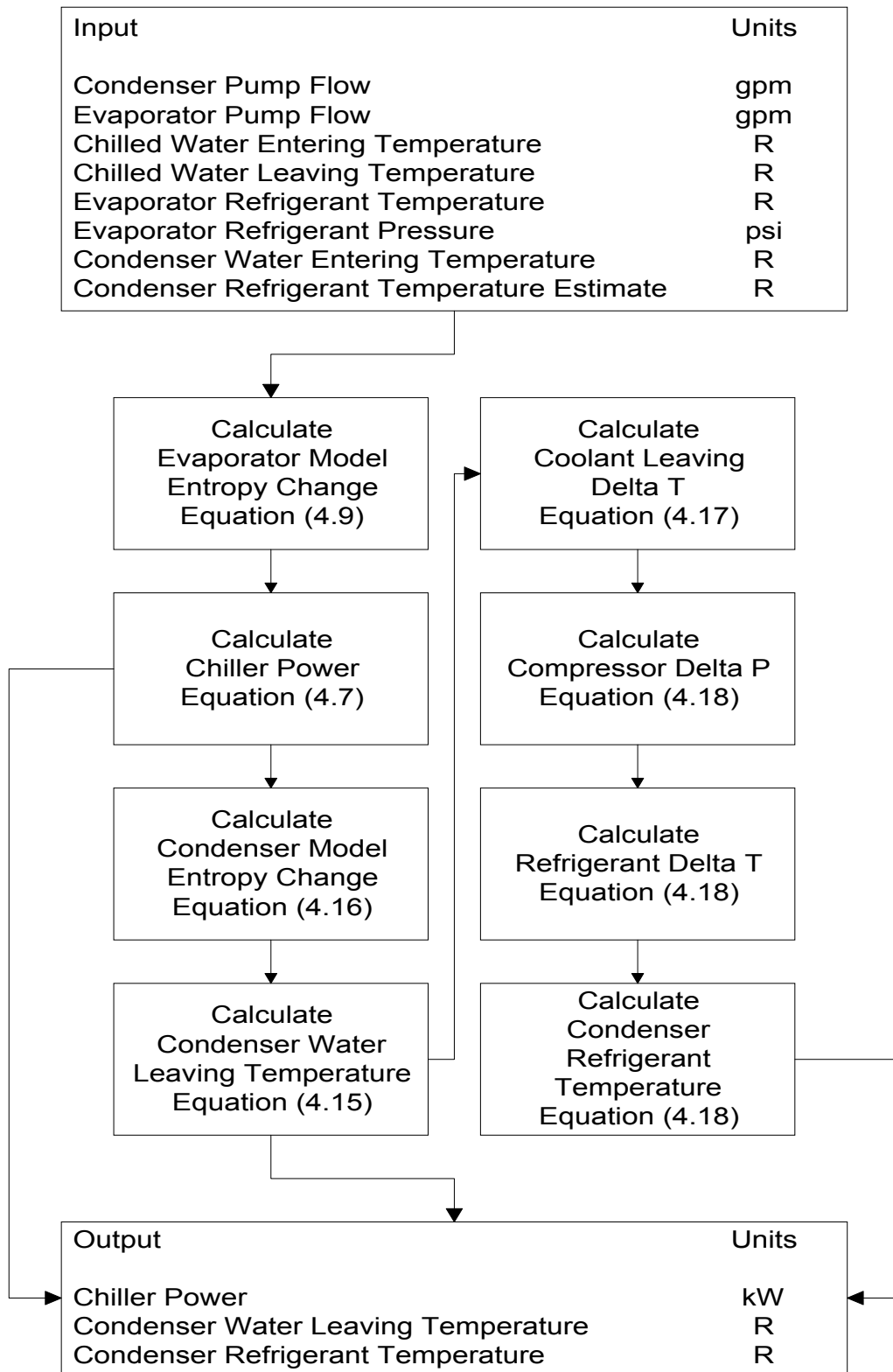


Figure 4.7. Chiller Model Flow Chart

## COOLING TOWER MODEL DEVELOPMENT



Figure 5.1. Test Facility Cooling Tower

Figure 5.1 shows the installed cross-flow cooling tower to be modeled. The first step in examining the performance of a cooling tower is to develop the mass balance equations for each flow stream:

$$\Delta \dot{m}_{\text{air}} = 0 = \dot{m}_{\text{a\_in}} - \dot{m}_{\text{a\_out}} \quad (5.1)$$

$$\Delta \dot{m}_{\text{water}} = 0 = \dot{m}_{\text{w\_in}} + \dot{m}_{\text{a\_in}} \omega_{\text{in}} - \dot{m}_{\text{w\_out}} - \dot{m}_{\text{a\_out}} \omega_{\text{out}} \quad (5.2)$$

Setting equation (5.1) equal to equation (5.2) and solving for  $\dot{m}_{\text{w\_out}}$  gives:

$$\dot{m}_{\text{w\_out}} = \dot{m}_{\text{w\_in}} + \dot{m}_{\text{a\_in}} (\omega_{\text{in}} - \omega_{\text{out}}) \quad (5.3)$$

Equation (5.3) is the governing mass balance equation for the cooling tower. The next step is to develop the energy balance equation for each flow stream:

$$\Delta E_{\text{air}} = 0 = (\dot{m}_{\text{a\_in}})(h_{\text{a\_in}}) - (\dot{m}_{\text{a\_out}})(h_{\text{a\_out}}) \quad (5.4)$$

$$\Delta E_{\text{water}} = 0 = (\dot{m}_{\text{w\_in}})(h_{\text{w\_in}}) - (\dot{m}_{\text{w\_out}})(h_{\text{w\_out}}) \quad (5.5)$$

The total energy balance for the cooling tower is:

$$\Delta E_{\text{total}} = 0 = \Delta E_{\text{water}} + \Delta E_{\text{air}} \quad (5.6)$$



Combining equations (5.3), (5.4), (5.5) and (5.6) gives:

$$\Delta E_{\text{total}} = 0 = \left( \dot{m}_{a\_in} \right) (h_{a\_in} - h_{a\_out}) + \left( \dot{m}_{w\_in} \right) (h_{w\_in}) - \left[ \dot{m}_{w\_in} + \dot{m}_{a\_in} (\omega_{in} - \omega_{out}) \right] (h_{w\_out}) \quad (5.7)$$

The enthalpy of the water can be expressed as:

$$h_w = c_{p\_w} (T_w) \quad (5.8)$$

Combining equations (5.7) and (5.8) and simplifying yields

$$\left( \dot{m}_{a\_in} \right) (h_{a\_out} - h_{a\_in}) - Y = \left( \dot{m}_{w\_in} \right) (c_{p\_w}) (T_{w\_in} - T_{w\_out}) \quad (5.9)$$

where

$$Y = \left( \dot{m}_{a\_in} \right) (\omega_{out} - \omega_{in}) (c_{p\_w}) (T_{w\_out})$$

For this cooling tower model, the assumptions made by Merkel in 1925 will be employed. These assumptions are:

1. Mass of water evaporated from the water stream is negligible.
2. Lewis number = 1.

Because the mass flow of water evaporated is on the order of 1% of the total mass flow entering the tower, the first Merkel assumption seems valid. Utilizing this

assumption, the  $Y$  term in equation (5.9) is reduced to zero. The assumption of a Lewis number equal to one means that there is a coefficient that utilizes the enthalpy difference as its driving force to account for both mass and sensible heat transfer (ASHRAE Handbook 1992). This allows equation (5.9) to be equated to

$$\dot{m}_{a\_in} (h_{a\_out} - h_{a\_in}) = \dot{m}_{w\_in} (c_{p\_w} (T_{w\_in} - T_{w\_out})) = K_m (h' - h_{air})_{avg} dV \quad (5.10)$$

where

$h'$  = enthalpy of air at the bulk water temperature, Btu/lb,

$h_{air}$  = enthalpy of air at the dry bulb temperature, Btu/lb,

$K_m$  = overall heat and mass transfer coefficient,

$dV$  = change in tower volume.

If a unit volume is considered, equation (5.10) becomes:

$$\left(\frac{\dot{m}}{\dot{m}_{a\_in}}\right)(h_{a\_out} - h_{a\_in}) = \left(\frac{\dot{m}}{\dot{m}_{w\_in}}\right)(c_{p\_w})(T_{w\_in} - T_{w\_out}) = K_m (h' - h_{air})_{avg} dA \quad (5.11)$$

The number of transfer units (NTU) is a term that is used to describe the physical size of the heat transfer area in a cooling tower. NTU is defined as:

$$NTU = \frac{K_m A}{\dot{m}_{a\_in}} \quad (5.12)$$

Inserting equation (5.12) into equation (5.11) and simplifying gives:

$$(h_{a\_out} - h_{a\_in}) = \left(\frac{\dot{m}}{\dot{m}_{a\_in}}\right) \left(\frac{\dot{m}}{\dot{m}_{w\_in}}\right) (c_{p\_w})(T_{w\_in} - T_{w\_out}) = NTU (h' - h_{air})_{avg} \quad (5.13)$$

Equation (5.13) is the governing equation for cooling tower performance. The value for NTU must be empirically determined. The value for NTU depends on the number of nodes used for analyzing the tower. A 10x10-node configuration was utilized for this model. The calculations begin in the upper left hand corner and proceed down and to the right. The enthalpy of the air changes from right to left while the temperature

of the water changes from top to bottom. Figure 5.2 shows a diagram of the cooling tower that shows how the air and water flows across the nodes.

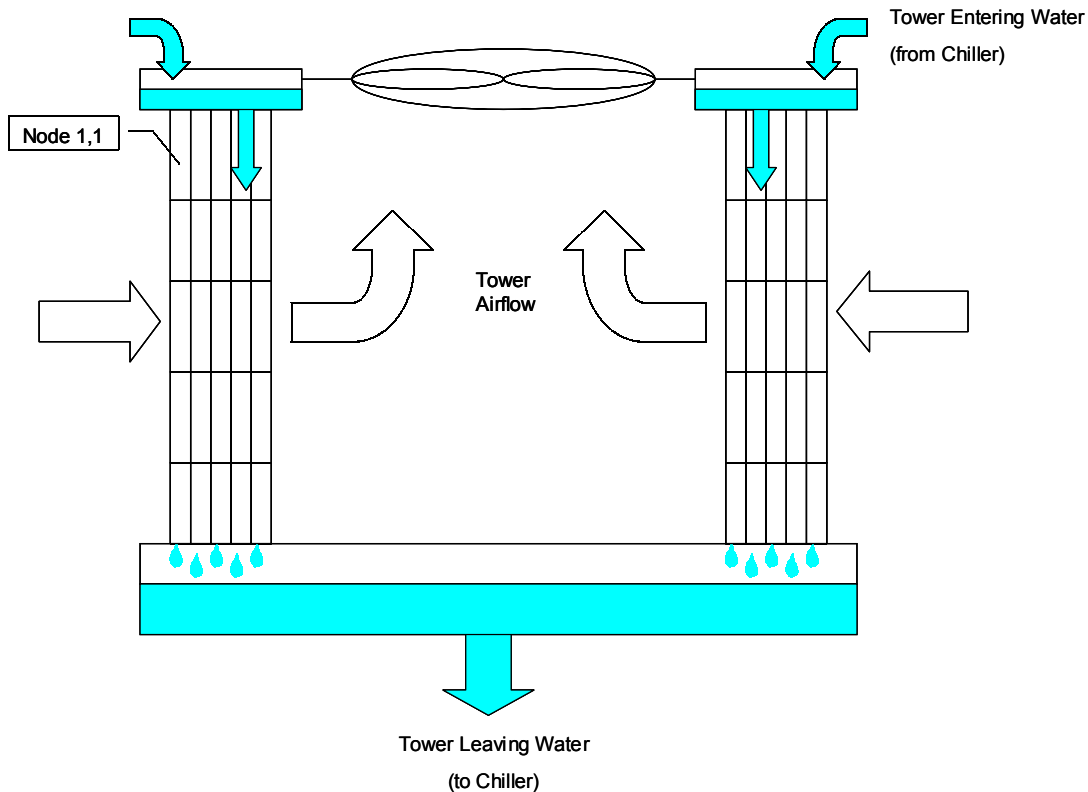


Figure 5.2. Cooling Tower Diagram

The entering water temperature for each node is equal to the leaving water temperature from the node above. Likewise, the entering air enthalpy is equal to the leaving air enthalpy from the node to the left. The entering air enthalpy and water temperature are used to estimate the change in air enthalpy and water temperature for the entering conditions. These values are then used to estimate the leaving air enthalpy and

water temperature. The leaving air enthalpy and water temperature are used to estimate the change in air enthalpy and water temperature for the leaving conditions. The changes in air enthalpy and water temperature for the entering and leaving conditions are averaged to provide the change across the node. Table 5.1 shows the set of values that are calculated in one node of the cooling tower model.

Table 5.1. Cooling Tower Node Values

<b>Node 1,1</b>			
<i>Name</i>	<i>Abbrev.</i>	<i>Value</i>	<i>Units</i>
Tower Entering Water Temperature	TWET	95	°F
Enthalpy of Entering Air	ha_in	42.63	Btu/lb
Saturation pressure of water @ TWET	Pw_ws	0.825	psi
Saturation humidity ratio @ TWET	Ws_wb	0.037	
Enthalpy of air @ TWET	h'_in	63.58	Btu/lb
Enthalpy Difference at inlet conditions	(h'-ha)in	20.95	Btu/lb
Water to Air Ratio	L/G	1.055	
Temperature Change based on inlet conditions	dTw inlet	3.06	°F
Enthalpy Change based on inlet conditions	dHah	3.22	Btu/lb
Tower Leaving Water Temperature	TWLT	91.94	°F
Enthalpy of Leaving Air	ha_out	45.85	Btu/lb
Saturation pressure of water @ TWLT	Pw_ws	0.750	psi
Saturation humidity ratio @ TWLT	Ws_wb	0.033	
Enthalpy of leaving air @ TWLT	h'_out	58.92	Btu/lb
Enthalpy Difference at outlet conditions	(h'-ha)out	13.08	Btu/lb
Average Enthalpy Difference	(h'-ha)av	17.01	Btu/lb
Change in Water Temperature	dTw	2.48	°F
Change in Air Enthalpy	dHah	2.62	Btu/lb

The value for NTU is determined by setting the boundary conditions to those established by the tower manufacturer and adjusting the value for NTU until the appropriate leaving water temperature is obtained. The NTU for the tower in this application is 14.60, or 0.1460 NTU/node. Once the NTU for the tower is determined,

the model can be used to predict the tower leaving water temperature for a variety of entering water temperatures and weather conditions. Figure 5.3 shows a comparison between the measured and calculated condenser water entering temperatures, i.e. the tower leaving water temperatures. These values were measured at the chiller and the temperature rise due to the cooling tower pump was neglected. The ideal CWET line represents the set of points that would be generated by a “perfect” tower model.

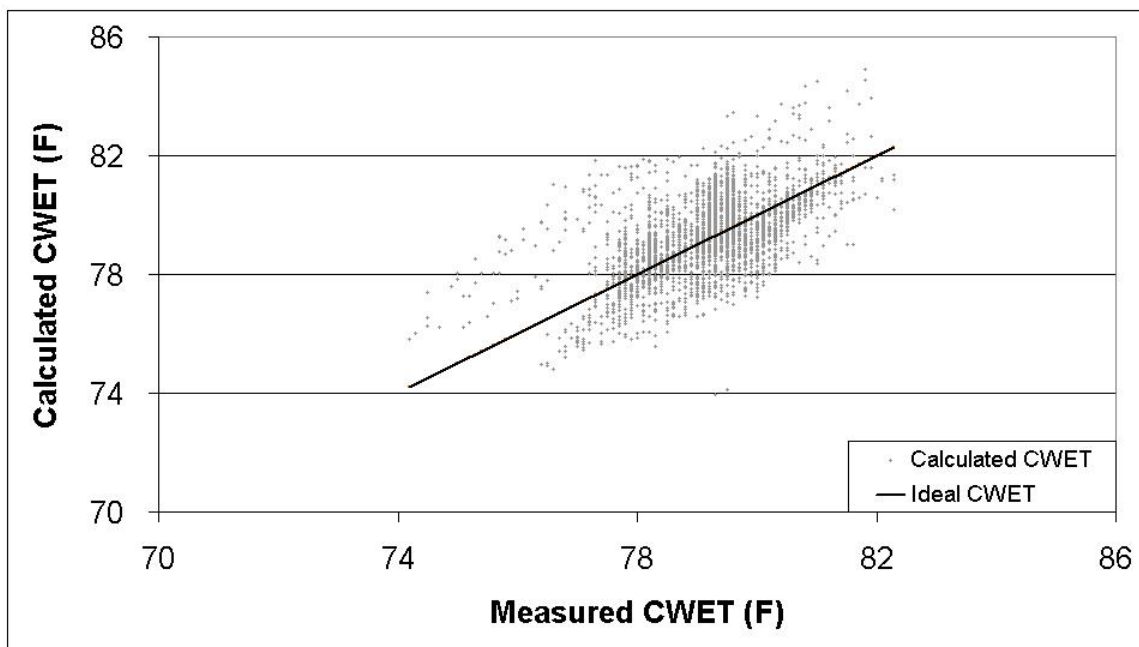


Figure 5.3. Condenser Water Entering Temperature Comparison

Figure 5.3 shows that the cooling tower model can calculate the condenser water entering temperature within  $\pm 4$  °F. During the process of coupling the chiller and cooling tower models, offsets will be employed to improve the accuracy of the model.

## COUPLING THE MODELS

In order to generate a complete chiller-tower model, the chiller and cooling tower models developed previously must be coupled together. The inputs and outputs of this model are shown in Table 6.1.

Table 6.1. Inputs and Outputs of Chiller-Tower Model

<i>Input</i>	<i>Units</i>	<i>Output</i>	<i>Units</i>
Cooling Tower Airflow	cfm	Condenser Refrigerant Temperature	°F
Condenser Pump Flow	gpm	Condenser Refrigerant Pressure	Psi
Evaporator Pump Flow	gpm	Condenser Water Entering Temperature	°F
Ambient Dry-bulb Temperature	°F	Condenser Water Leaving Temperature	°F
Ambient Wet-bulb Temperature	°F	Chiller Power	kW
Chilled Water Entering Temperature	°F	Cooling Tower Fan Power	kW
Chilled Water Leaving Temperature	°F	Condenser Pump Power	kW
Evaporator Refrigerant Temperature	°F		
Evaporator Refrigerant Pressure	psi		

The chiller model calculates the condenser refrigerant temperature, condenser refrigerant pressure, condenser leaving water temperature, and chiller power. The cooling tower model calculates the condenser entering water temperature. The cooling tower fan power and condenser pump power are calculated from the pump flow and airflow inputs using the fan laws. An iterative method was employed, beginning with the chiller model, measured data for the inputs, and initial estimate values for the cooling tower leaving water temperature, condenser refrigerant temperature, and change in pressure across the compressor. The condenser leaving water temperature is then used

for the cooling tower entering water temperature. The leaving water temperature from the cooling tower model is used for the entering condenser coolant temperature for a subsequent chiller iteration. In this way, the cooling tower models and chiller model are coupled to create a chiller-tower model that will investigate the concomitant performance of both systems. Figure 6.1 shows a comparison of the calculated chiller plant power with the measured plant power. Also shown on this graph is the ideal plant power line. The data points were calculated using inputs measured every fifteen minutes over the period from 5/13/03 to 6/30/03. There were 4,101 total input points that were used in this calculation. The chiller contributes 75% of the energy consumed by the chiller plant, so the chiller plant power comparison is closely related in shape to the chiller model curve shown in Figure 4.3. Figure 6.1 shows that the model without the offsets can predict the power consumption of the chiller plant within  $\pm 5\%$  over the entire range of the measured power.



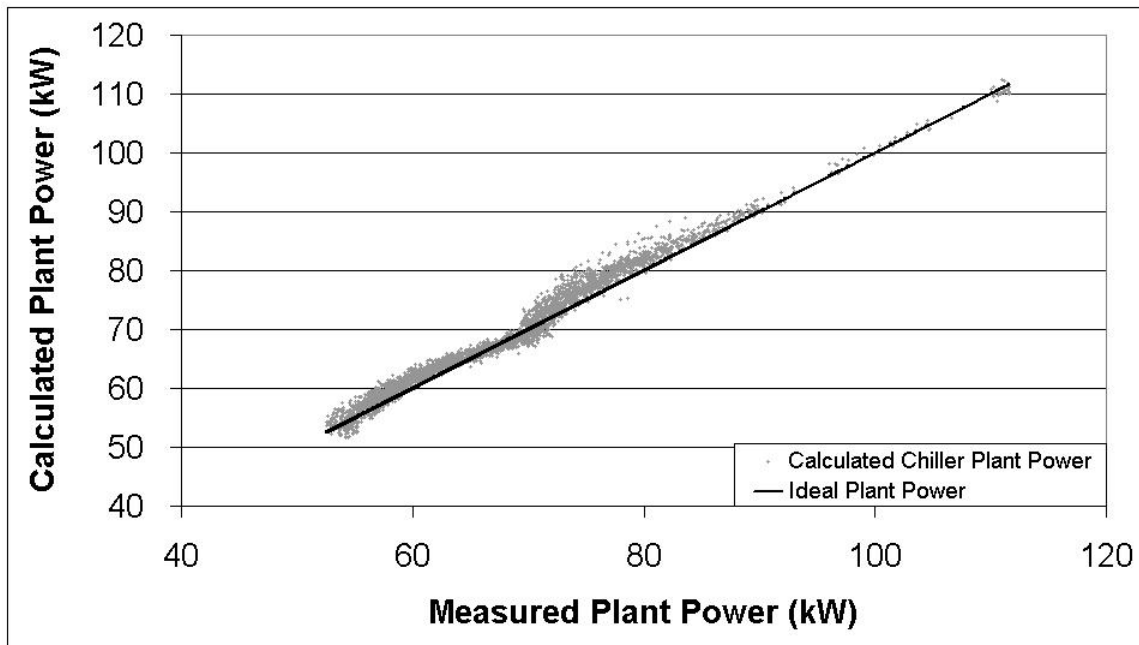


Figure 6.1. Chiller Plant Power Comparison (without offsets)

In order to better fit the curve to the data, an offset term was employed for each of the outputs of the chiller-tower model. The offsets were determined by subtracting the calculated value from the measured value for each output. The offset was then defined as the average of the difference for each term. The offset for each component is shown in Table 6.2 below.

Table 6.2. Output Offsets

<i>Offset</i>	<i>Condenser Water Entering Temp (F)</i>	<i>Condenser Water Leaving Temp (F)</i>	<i>Condenser Refrigerant Temp (F)</i>	<i>Condenser Refrigerant Pressure (psi)</i>	<i>Compressor Power (kW)</i>
Maximum Offset	5.39	5.67	6.94	12.32	3.54
Minimum Offset	-4.55	-3.86	-3.23	-6.18	-6.89
Average Offset	-0.21	0.30	0.78	0.81	-1.13

Utilizing the average offsets for each component, the chiller-tower model is run again for the same data set. The results of the model, including the offsets, are shown in Figure 6.2. The model with the offsets included is capable of calculating the plant power within  $\pm 3\%$  of the ideal plant power line. This chart shows that the coupling the chiller and cooling tower models produces a reasonably accurate chiller-tower model. This model will be used with an optimization strategy to minimize the energy consumption of the chiller plant.

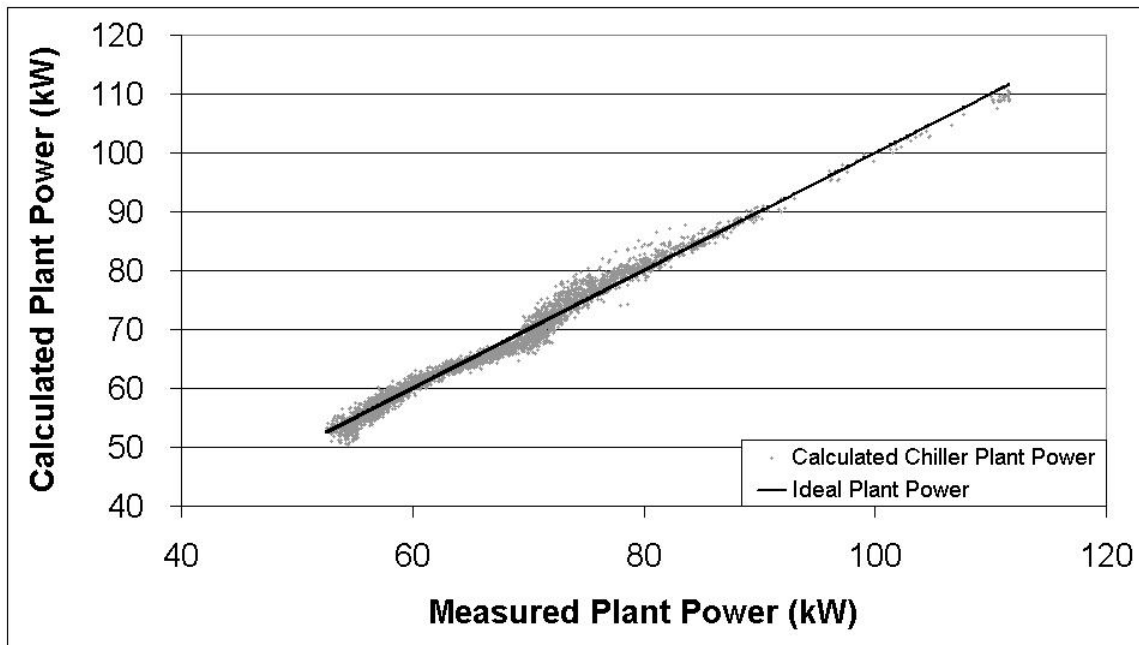


Figure 6.2. Chiller Plant Power Comparison (with offsets)

Figures 6.3 through 6.7 show the error associated with each calculated output. Taking the difference between the calculated value and the measured value generated these errors. The spread between the maximum and minimum errors was divided into

one hundred bins. The number of error points in each bin was summed and then plotted versus the bin value to generate a bell curve to describe the error associated with each measurement. Table 6.3 shows the standard deviation associated with each bell curve.

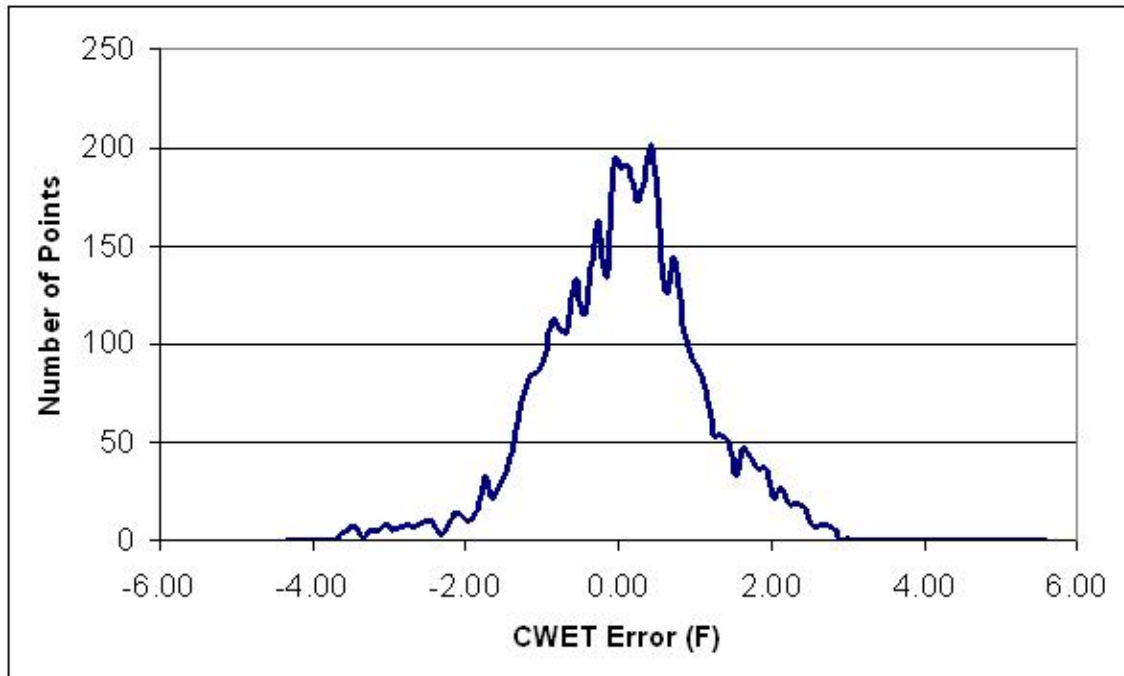


Figure 6.3. Condenser Water Entering Temperature Error

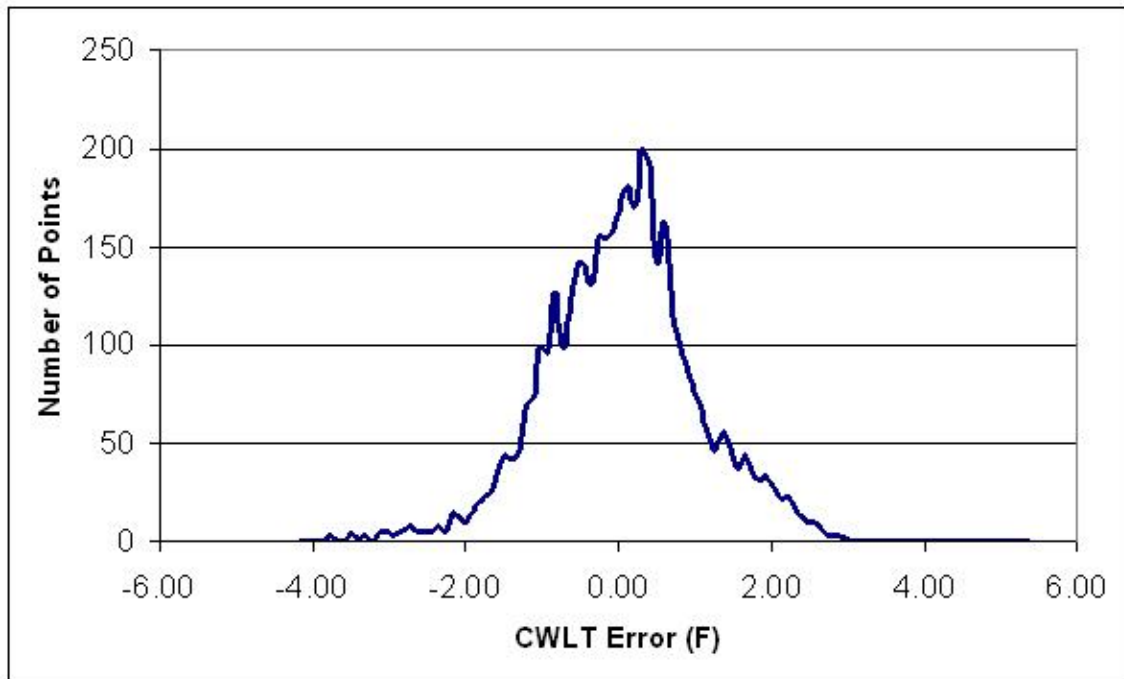


Figure 6.4. Condenser Water Leaving Temperature Error

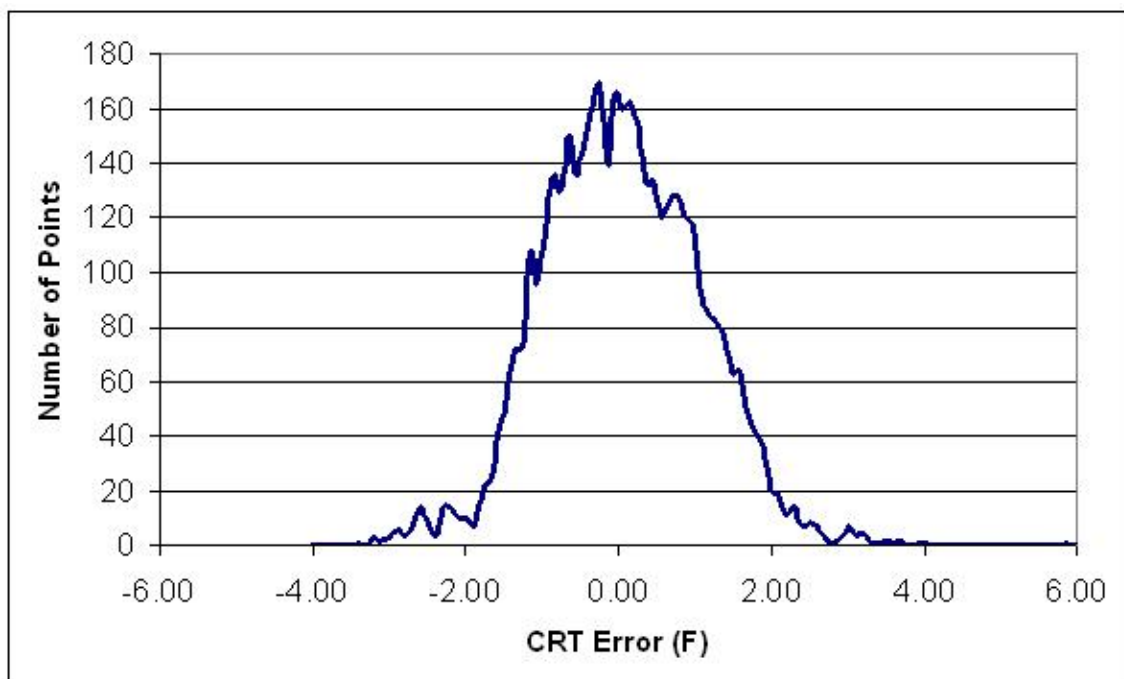


Figure 6.5. Condenser Refrigerant Temperature Error

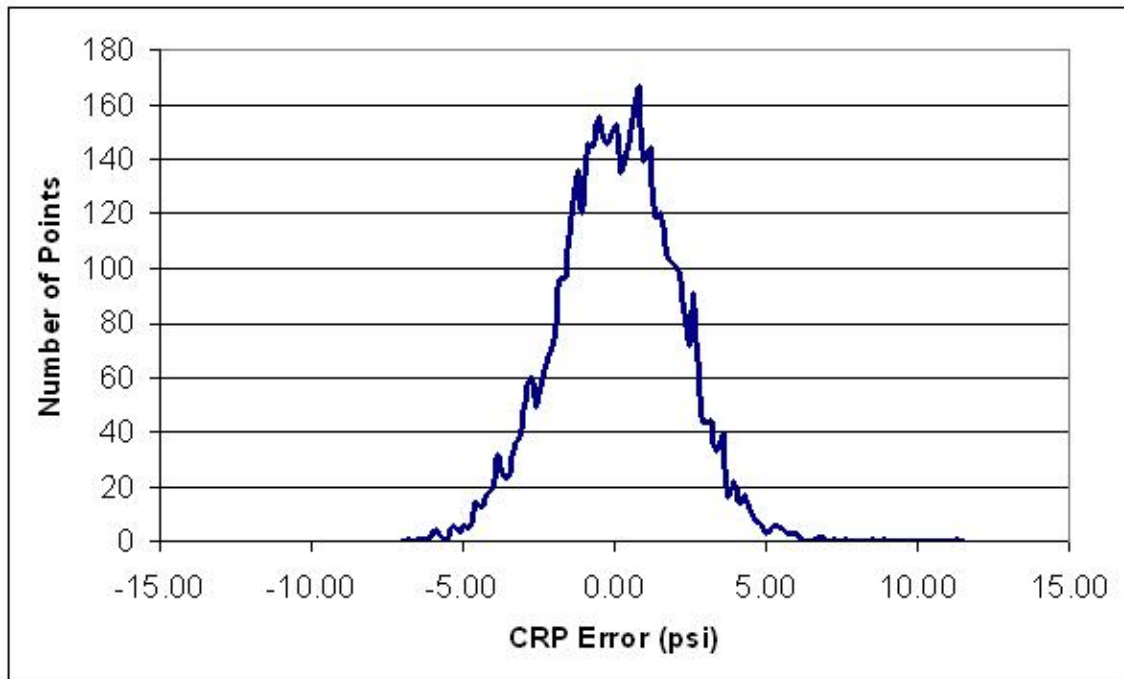


Figure 6.6. Condenser Refrigerant Pressure Error

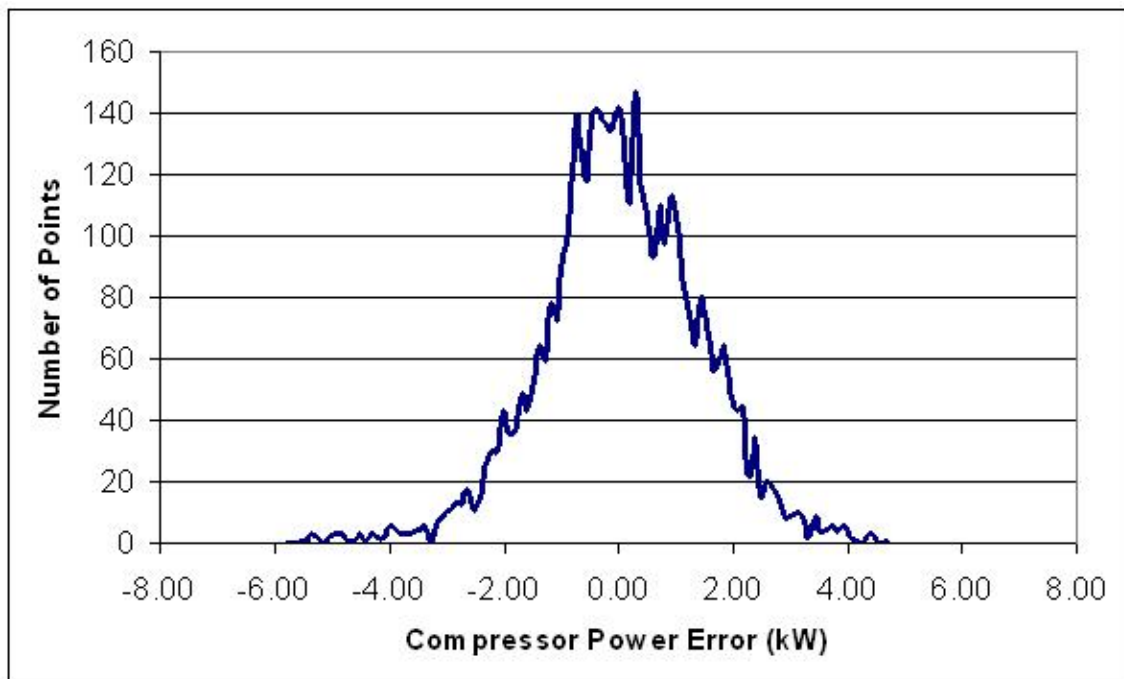


Figure 6.7. Compressor Power Error

Table 6.3. Standard Deviations for Each Component

<i>Component</i>	<i>Standard Deviation</i>	<i>Units</i>
Condenser Water Entering Temperature	1.04	F
Condenser Water Leaving Temperature	1.01	F
Condenser Refrigerant Temperature	1.04	F
Condenser Refrigerant Pressure	2.01	psi
Compressor Power	1.38	kW

Since the standard deviation of the error of each calculated value is within the error bands of the device used to measure these values, the model is capable of accurately predicting the performance of the system.

## OPTIMIZATION STRATEGY AND ANALYSIS

In order to optimize the chiller plant, the chiller-tower model is utilized to determine the optimal cooling tower fan speed and condenser water pump flow. The cooling tower fan speed and condenser pump flow are the only two inputs that are directly related to the optimization of the chiller plant from the condenser side. The remaining chiller-tower model inputs pertain either to weather conditions or to building load and are independent with respect to the varying of condenser water flow rate.

The sum of the chiller power, cooling tower fan power, and condenser water pumping power is minimized using an iterative method with the cooling tower fan speed and condenser pump flow as the variables. This is accomplished by using a mathematical equation solver that performs the iterations using a quasi-Newtonian method to achieve the minimum value. The cooling tower fan speed is first solved for the minimum value, then the condenser pump flow. A second iteration of the cooling tower fan speed and condenser pump flow is performed to ensure that the true minimum value is obtained. Figure 7.1 shows a comparison of the current simulated chiller plant power to the optimized chiller plant power over the period of time between 5/17/03 and 5/27/03. Also shown is the power difference, i.e. power savings, realized by the installation of the optimized system.

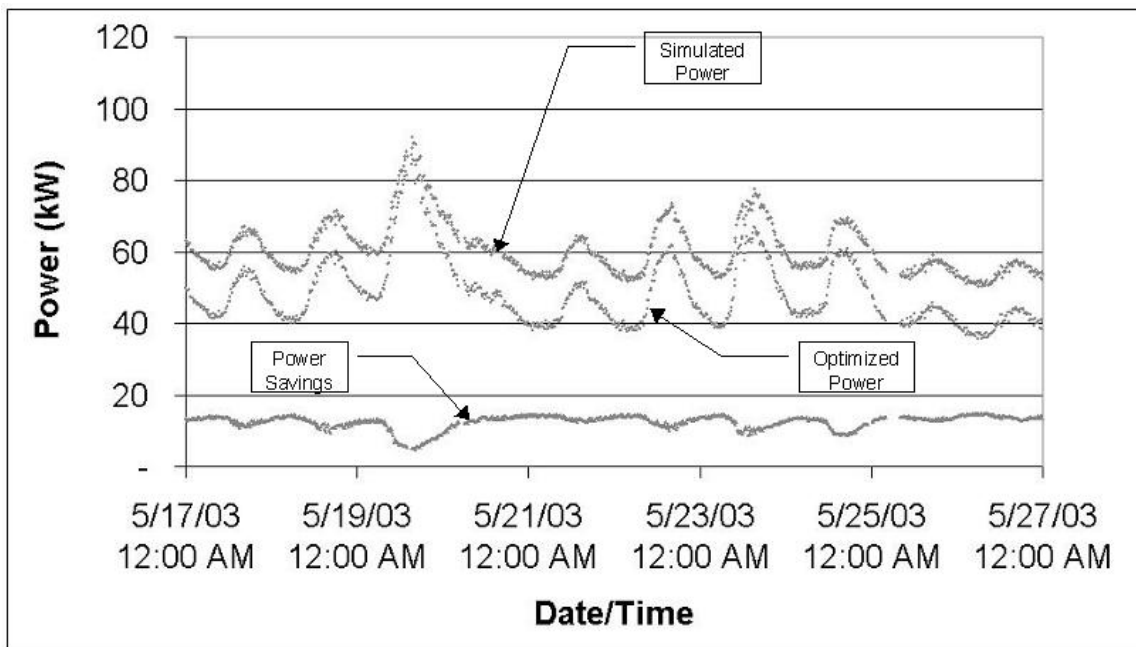


Figure 7.1. Optimized Chiller Plant Power Comparison

The optimizer returns the ideal values for the cooling tower fan speed and condenser water pump flow as well as the other outputs supplied by the simulator. In order to optimize the real system, a correlation between the optimized cooling tower fan speed and the condenser water pump flow must be implemented. One of the most popular methods for controlling cooling tower fan variable-frequency drives (VFD) involves a cooling tower leaving water temperature setpoint. This setpoint, typically an operator-specified value, is subtracted from the measured cooling tower leaving water temperature to provide a differential for controlling the cooling tower VFD. The control loop for a typical cooling tower fan VFD is shown in Figure 7.2.



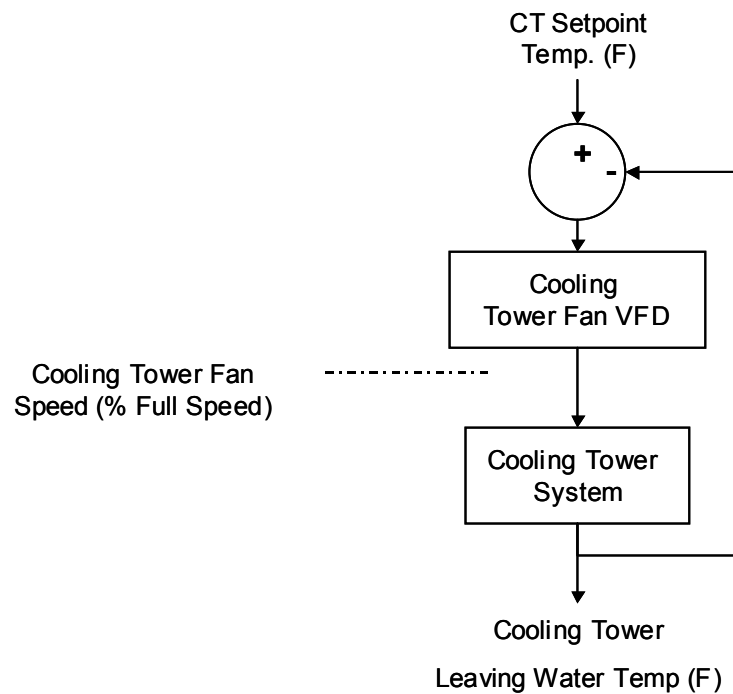


Figure 7.2. Typical Cooling Tower Fan VFD Control Loop

Since this type of VFD control is currently installed on the system and the building owner does not want to change the operation of a working device, the setpoint becomes the only variable that can be adjusted with regard to the cooling tower fan controls. In order to exercise the abilities of the VFD, the cooling tower setpoint must be above the wet-bulb temperature. If the cooling tower setpoint is below the wet-bulb temperature, the cooling tower fan will run full speed in an effort to reach a tower leaving water temperature that is thermodynamically impossible. It has been suggested that setting the cooling tower setpoint to a constant value above the wet-bulb temperature will provide “near optimal” tower operation (Burger 1993, Hartman 2001). The output data provided by the chiller-tower model optimization shows the ideal

condenser entering water temperature. The optimized condenser entering water temperature should be used as the setpoint for the cooling tower fan VFD. There is a very strong correlation between the wet-bulb temperature and the ideal condenser entering water temperature. This correlation is shown in Figure 7.3.

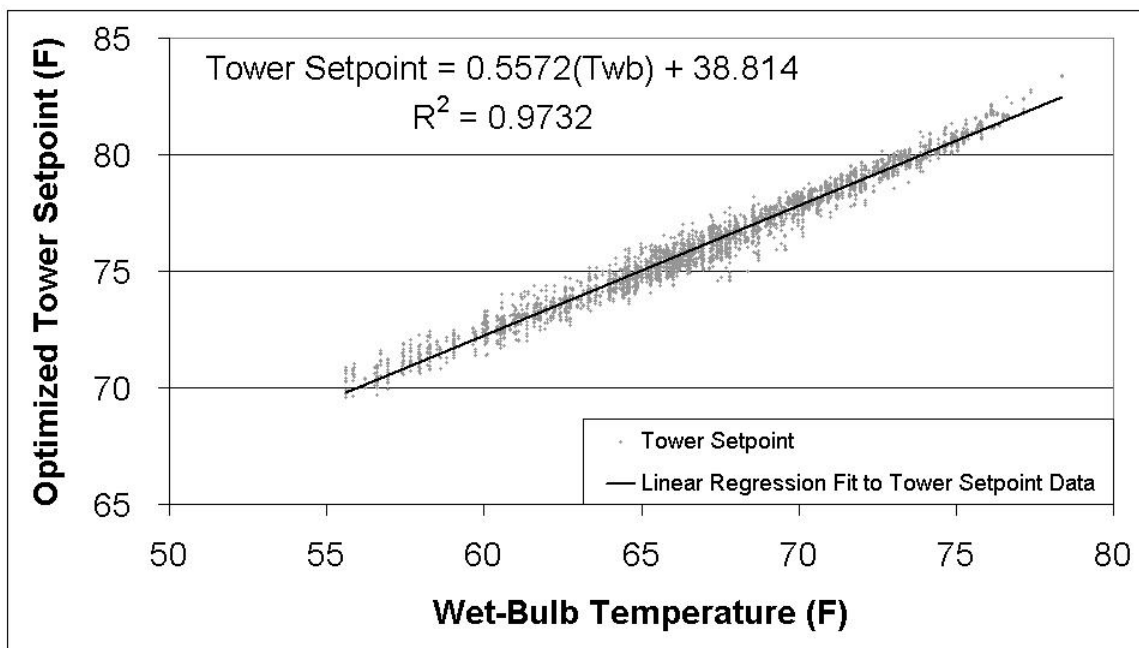


Figure 7.3. Cooling Tower Setpoint vs. Wet-Bulb Temperature

This correlation shows that the building automation software can be used to calculate the ideal cooling tower setpoint using the temperature and humidity measurements. The optimum heat exchanger effectiveness occurs when the thermal capacities of each fluid stream are equal (Whillier 1976). For the cooling tower, this means that there is an optimum ratio of mass water flow to mass airflow, or more specifically, an ideal condenser water pump speed versus cooling tower fan speed.

Indeed, comparing the optimal cooling tower fan speed to the ideal condenser water pump speed shows a strong correlation between these two values. This comparison is shown in Figure 7.4. The R-square value for the linear regression fit is 0.88. This is primarily due to the effect that air density has on the relationship between cooling tower fan speed and cooling tower mass airflow. An R-square value of 0.98 can be obtained by adding a wet-bulb correction factor. However, the added complexity results in a three percent change in the energy savings, which is not significant enough to warrant the added complexity.

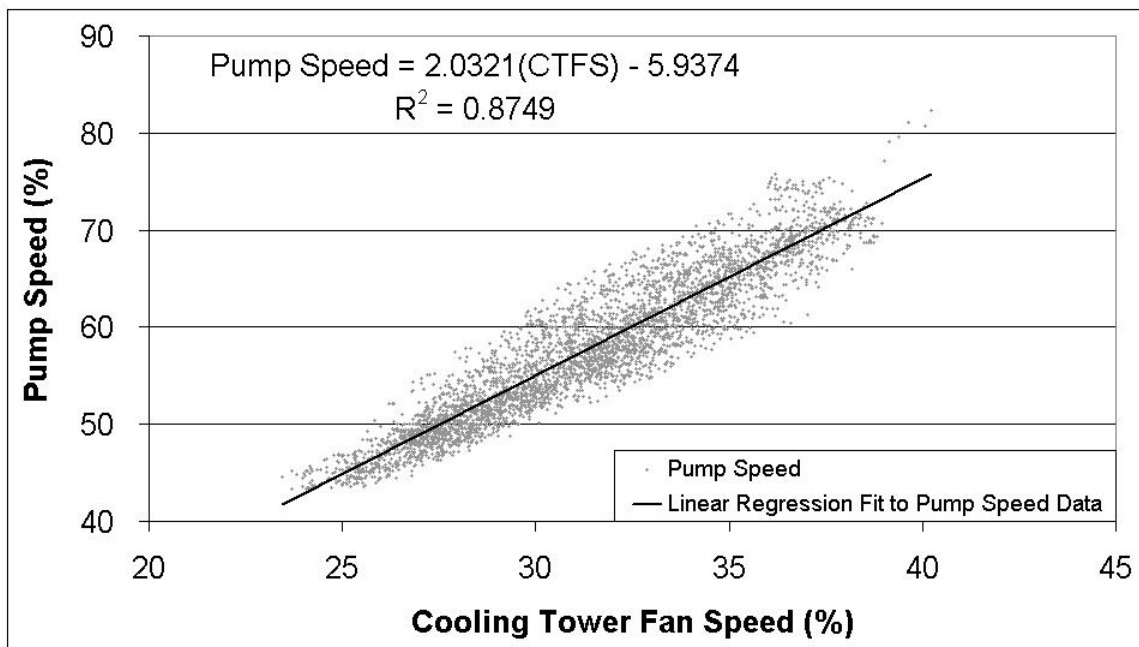


Figure 7.4. Condenser Water Pump Speed vs. Cooling Tower Fan Speed

Utilizing the correlations developed in Figures 7.3 and 7.4 will result in a “quasi-optimal” operation of the chiller plant. In order to define the losses incurred by using the

“quasi-optimal” control, the chiller-tower model is modified to calculate the cooling tower fan speed given a setpoint. This setpoint is determined from the wet-bulb temperature, which is calculated from the temperature and relative humidity inputs. The condenser pump flow is no longer an input, but is calculated from the cooling tower fan speed. A diagram of the quasi-optimal control loop is shown in figure 7.5.

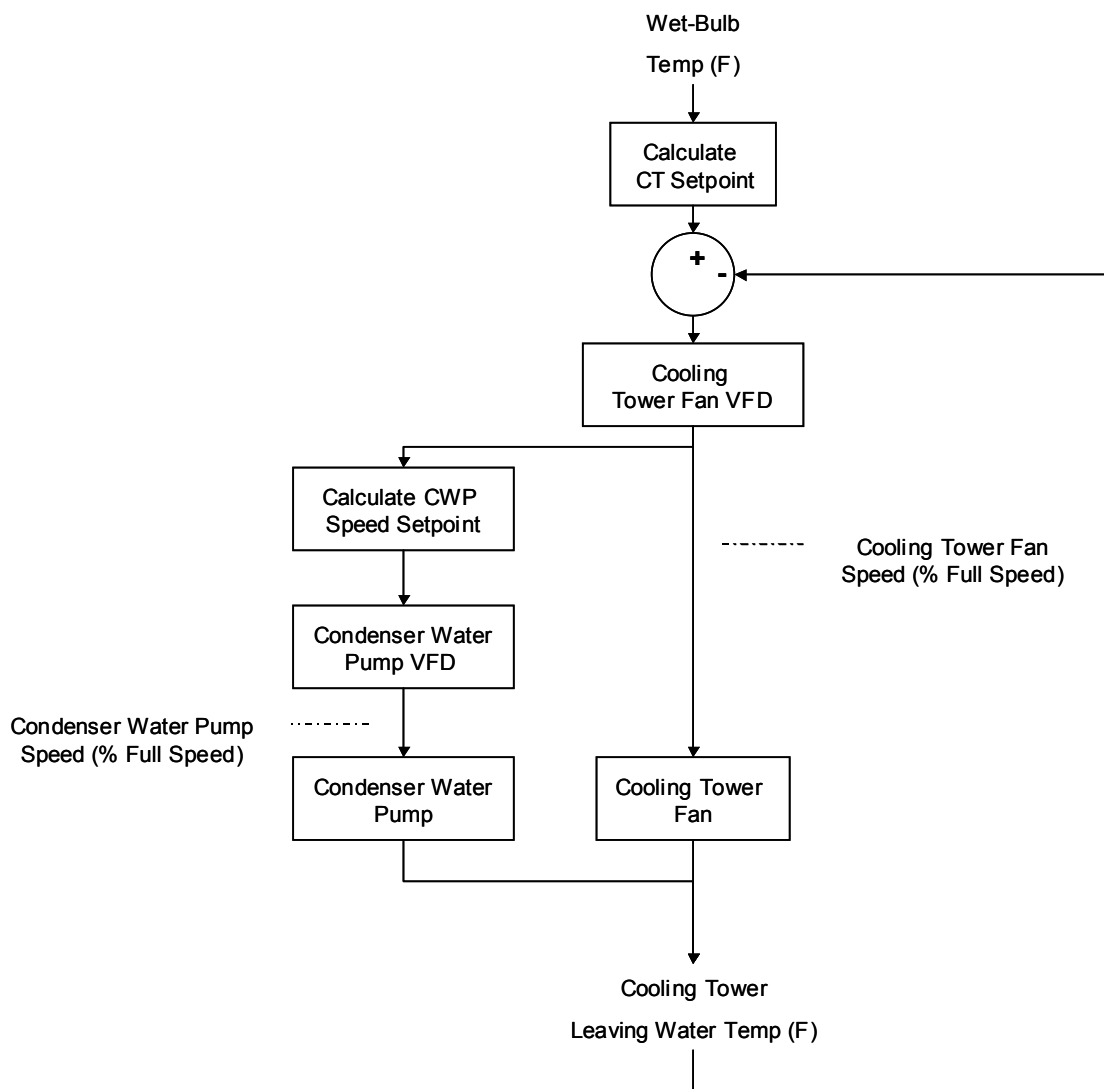


Figure 7.5. Quasi-Optimal Control Loop

The results of the “quasi-optimal” operation versus the optimal operation are shown in Figure 7.6. The “quasi-optimal” operation proposed yields a power consumption that is approximately 1% higher than a truly optimal operation.

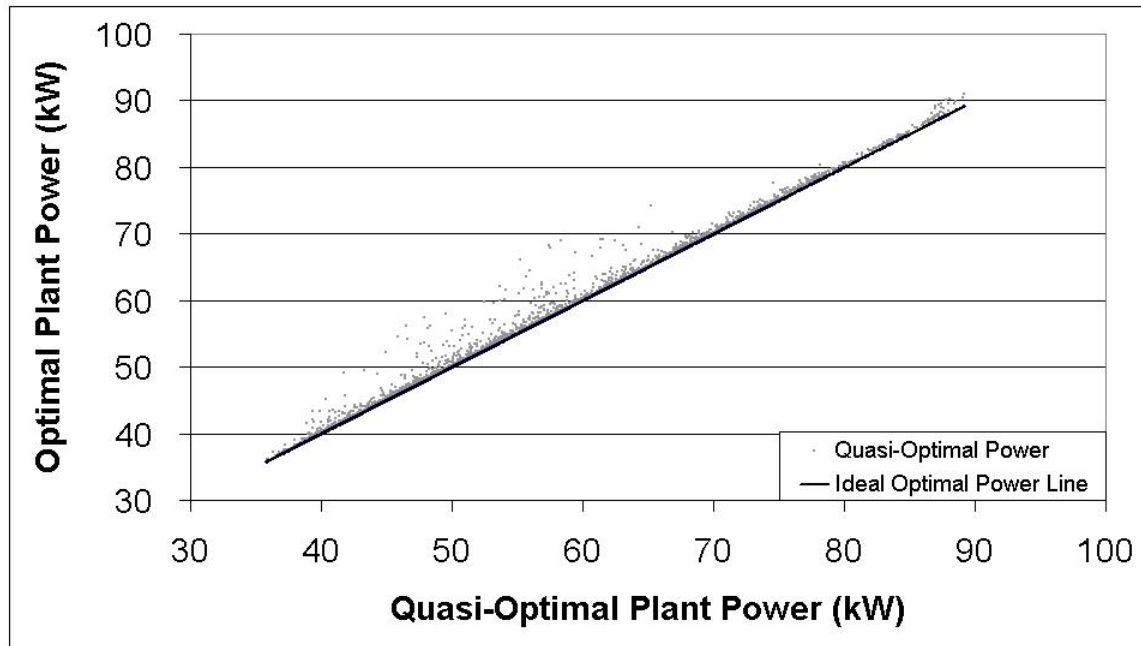


Figure 7.6. Quasi-Optimal Chiller Plant Power Comparison

Implementing new method for controlling the cooling tower setpoint and the condenser water pump flow shows an 18% average reduction in chiller plant power.

## CONCLUSIONS

The development of the combined chiller-tower model allows the opportunity to explore what will occur in a real system without endangering the equipment in that system. In this case, the chiller-tower model was used to predict the performance of the chiller plant under the conditions of variable condenser water flow rate and variable tower airflow. The model is able to estimate the energy consumption with enough accuracy to ensure that energy savings over 5% of the current total will indeed occur. However, this model will need some refinement before it can be used to definitively predict energy savings.

One task that was not undertaken was the validation of the optimized model. This is due to the lack of an existing VFD on the condenser water pumps. The primary goal of this thesis was to develop a thermodynamic chiller-tower model that could be used to predict the energy savings allowed by a retrofit. This was to provide an economic justification for the retrofit without actually having to implement the retrofit. In to truly validate the model's optimization capability, the retrofit must be made to an existing system and post-retrofit measurements taken.

Another particular weakness of this combined chiller-tower model is the cooling tower model that was employed. This model is very good for systems in which the cooling tower is matched to the chiller. In this situation the cooling tower capacity was twice the capacity of the one chiller that normally operates. This resulted in tower water flow rates that were one-half that for which the cooling tower was designed. Further

reducing the tower water flow rate affects the tower nozzles' ability to disperse the water evenly over the tower. This can result in a lower effective evaporation surface area, which would effectively reduce the tower NTU. There was no simple correlation found between the tower NTU and any of the independent variables. Because many chiller plants are designed with one large cooling tower, the ability to model the effects of a cooling tower at less than 50% tower airflow and water flow rates is very valuable.

A third area that deserves some attention is the area of controls. For simplicity's sake, the chiller plant in this situation is controlled using coupled single-input-single-output loops. The truly optimal relationship between the condenser pump flow and cooling tower fan speed may be realized by utilizing a multiple-input-multiple-output control sequence.

The combined chiller-tower model shows that there are two simple correlations that can be used to optimize a chiller plant. The first is the correlation between cooling tower setpoint and the wet-bulb temperature. The second is the correlation between the cooling tower fan speed and the condenser water pump speed. These two correlations can be used to provide "quasi-optimal" operation of a chiller plant.

## REFERENCES

- Aoyama, M. and M. Izushi. 1990. Continuous capacity control type screw chiller unit. *Hitachi Review* 39(3):149-154.
- ASHRAE. 1992. *ASHRAE Handbook – HVAC Systems and Equipment*. Atlanta: American Society of Heating, Refrigerating and Air-Conditioning Engineers, Inc.
- Austin, S.B. 1991. Optimum chiller loading. *ASHRAE Journal* 33(7):40-43.
- Braun, J.E. 1988. Methodologies for the design and control of central cooling plants. Ph.D. dissertation, University of Wisconsin-Madison.
- Braun, J.E. and G.T. Diderrich. 1990. Near-optimal control of cooling towers for chilled-water systems. *ASHRAE Transactions* 96(2):806-813.
- Burger, R. 1993. Wet bulb temperature: The misunderstood element. *HPAC Engineering* 65(9):29-34.
- Cascia, M.A. 2000. Implementation of a near-optimal global set point control method in a DDC controller. *ASHRAE Transactions* 106(1):249-263.
- Chua, H.T., K.C. Ng and J.M. Gordon. 1996. Experimental study of the fundamental properties of reciprocating chillers and their relation to thermodynamic modeling and chiller design. *International Journal of Heat and Mass Transfer* 39(11):2195-2204.
- Flake, B.A., J.W. Mitchell and W.A. Beckman. 1997. Parameter estimation for multiresponse nonlinear chilled-water plant models. *ASHRAE Transactions* 103(1):470-485.
- Gibson, G.L. 1997. A supervisory controller for optimization of building central cooling systems. *ASHRAE Transactions* 103(1):486-493.
- Gordon, J.M. and K.C. Ng. 1995. Predictive and diagnostic aspects of a universal thermodynamic model for chillers. *International Journal of Heat and Mass Transfer* 38(5):807-818.
- Gordon, J.M. and K.C. Ng. 2000. *Cool Thermodynamics*. London: Cambridge International Science Publishing. 2000.



- Gordon, J.M., K.C. Ng, H.T. Chua. 1995. Centrifugal chillers: Thermodynamic modeling and a diagnostic case study. *International Journal of Refrigeration* 18(4):253-257.
- Gordon, J.M., K.C. Ng, H.T. Chua and C.K. Lim. 2000. How varying condenser coolant flow rate affects chiller performance: Thermodynamic modeling and experimental confirmation. *Applied Thermal Engineering* 20(13):1149-1159.
- Hartman, T. 2001. All-variable speed centrifugal chiller plants. *ASHRAE Journal* 43(9):43-51.
- He, X., S. Liu, H.H. Asada and H. Itoh. 1998. Multivariable control of vapor compression systems. *HVAC&R Research* 4(3):205-230.
- Henze, G.P., R.H. Dodier and M. Krarti. 1997. Development of a predictive optimal controller for thermal energy storage systems. *HVAC&R Research* 3(3):233-264.
- Kirsner, W. 1996. 3 GPM/Ton condenser water flow rate: Does it waste energy? *ASHRAE Journal* 38(2):63-69.
- Lau, A.S., W.A. Beckman and J.W. Mitchell. 1985. Development of computerized control strategies for a large chilled water plant. *ASHRAE Transactions* 91(1B):766-780.
- Ng, K.C., H.T. Chua, W. Ong, S.S. Lee and J.M. Gordon. 1997. Diagnostics and optimization of reciprocating chillers: Theory and experiment. *Applied Thermal Engineering* 17(3):263-276.
- Rolfsman, L. and S. Wihlborg. 1996. Screw compressor capacity regulated by stepless speed control. *ABB Review* (4):18-23.
- Schwedler, M. 1998. Take it to the limit...Or just halfway? *ASHRAE Journal* 40(7):32-39.
- Schwedler, M. and B. Bradley. 2001. Uncover the hidden assets in your condenser water system. *HPAC Engineering* 73(11):68,75.
- Stagg, J. Trane – Tracer Summit Applications Technician. Fort Worth, Texas. Personal communication concerning the communications and storage capabilities of the Trane Tracer BCUs.
- Stout, M.R., Jr. and J.W. Leach. 2002. Cooling tower fan control for energy efficiency. *Energy Engineering* 99(1):7-31.

Van Dijk, H. 1985. Investment in cooling tower control pays big dividends. *Process Engineering* 66(10):57, 59-60.

Weber, E.D. 1988. Modeling and generalized optimization of commercial building chiller/cooling tower systems. Master's thesis, Georgia Institute of Technology.

Whillier, A. 1976. A fresh look at the calculation of performance of cooling towers. *ASHRAE Transactions* 82(1):269-282.

## APPENDIX A

### COMPLETE CHILLER DERIVATION

The First Law equation that describes the refrigerant-side operation of a chiller is

$$\Delta E = 0 = Q_{\text{cond}} + Q_{\text{cond}}^{\text{leak}} - Q_{\text{evap}} - Q_{\text{evap}}^{\text{leak}} - P_{\text{in}} + Q_{\text{comp}}^{\text{leak}} \quad (\text{A.1})$$

where

$Q_{\text{cond}}$  = heat transfer in the condenser, kW,

$Q_{\text{cond}}^{\text{leak}}$  = heat transfer from the condenser piping to the environment, kW,

$Q_{\text{evap}}$  = heat transfer in the evaporator, kW,

$Q_{\text{evap}}^{\text{leak}}$  = heat transfer from the evaporator piping to the environment, kW,

$P_{\text{in}}$  = compressor power input, kW,

$Q_{\text{comp}}^{\text{leak}}$  = heat transfer from the compressor to the environment, kW.

The Second Law equation is

$$\Delta S = 0 = \left( \frac{Q_{\text{cond}} + Q_{\text{cond}}^{\text{leak}}}{T_{\text{cond}}^{\text{refr}}} \right) - \left( \frac{Q_{\text{evap}} + Q_{\text{evap}}^{\text{leak}}}{T_{\text{evap}}^{\text{refr}}} \right) - \Delta S_{\text{internal}} \quad (\text{A.2})$$

where

$T_{\text{cond}}^{\text{refr}}$  = temperature of the condensing refrigerant, R,

$T_{\text{evap}}^{\text{refr}}$  = temperature of the evaporating refrigerant, R,

$\Delta S_{\text{int ernal}}$  = internal entropy production, kW/R.

Solving equation (A.2) for  $Q_{\text{cond}}$  gives the following:

$$Q_{\text{cond}} = \frac{T_{\text{cond}}^{\text{refr}}}{T_{\text{evap}}^{\text{refr}}} (Q_{\text{evap}} + Q_{\text{evap}}^{\text{leak}}) + T_{\text{cond}}^{\text{refr}} \Delta S_{\text{int ernal}} - Q_{\text{condenser}}^{\text{leak}} \quad (\text{A.3})$$

Inserting  $Q_{\text{cond}}$  obtained in equation (A.3) into equation (A.1) yields:

$$0 = \frac{T_{\text{cond}}^{\text{refr}}}{T_{\text{evap}}^{\text{refr}}} (Q_{\text{evap}} + Q_{\text{evap}}^{\text{leak}}) + T_{\text{cond}}^{\text{refr}} \Delta S_{\text{int ernal}} - Q_{\text{cond}}^{\text{leak}} + Q_{\text{cond}}^{\text{leak}} - Q_{\text{evap}} - Q_{\text{evap}}^{\text{leak}} - P_{\text{in}} + Q_{\text{comp}}^{\text{leak}} \quad (\text{A.4})$$

The  $Q_{\text{cond}}^{\text{leak}}$  term cancels out and equation (A.4) is solved for  $P_{\text{in}}$  to obtain:

$$P_{\text{in}} = \frac{T_{\text{cond}}^{\text{refr}}}{T_{\text{evap}}^{\text{refr}}} (Q_{\text{evap}} + Q_{\text{evap}}^{\text{leak}}) + T_{\text{cond}}^{\text{refr}} \Delta S_{\text{int ernal}} - Q_{\text{evap}} - Q_{\text{evap}}^{\text{leak}} + Q_{\text{comp}}^{\text{leak}} \quad (\text{A.5})$$

By combining the  $Q_{\text{evap}}$  and  $Q_{\text{evap}}^{\text{leak}}$  terms, equation (A.5) becomes:

$$P_{\text{in}} = Q_{\text{evap}} \left( \frac{T_{\text{cond}}^{\text{refr}}}{T_{\text{evap}}^{\text{refr}}} - 1 \right) + Q_{\text{evap}}^{\text{leak}} \left( \frac{T_{\text{cond}}^{\text{refr}}}{T_{\text{evap}}^{\text{refr}}} - 1 \right) + Q_{\text{evap}}^{\text{leak}} + T_{\text{cond}}^{\text{refr}} \Delta S_{\text{int ernal}} \quad (\text{A.6})$$

Dividing both sides of equation (A.6) by  $Q_{\text{evap}}$  gives:

$$\frac{P_{\text{in}}}{Q_{\text{evap}}} = -1 + \frac{T_{\text{cond}}^{\text{refr}}}{T_{\text{evap}}^{\text{refr}}} + \frac{Q_{\text{evap}}^{\text{leak}}}{Q_{\text{evap}}} \left( \frac{T_{\text{cond}}^{\text{refr}}}{T_{\text{evap}}^{\text{refr}}} - 1 \right) + \frac{Q_{\text{comp}}^{\text{leak}}}{Q_{\text{evap}}} + \frac{T_{\text{cond}}^{\text{refr}} \Delta S_{\text{int ernal}}}{Q_{\text{evap}}} \quad (\text{A.7})$$

The coefficient of performance (COP) of a chiller is defined as:

$$\text{COP} = \frac{Q_{\text{evap}}}{P_{\text{in}}} \quad (\text{A.8})$$

Inserting the reciprocal of equation (A.8) into equation (A.7) and moving the  $Q^{\text{leak}}$  terms to the end of the equation gives:

$$\frac{1}{\text{COP}} = -1 + \frac{T_{\text{cond}}^{\text{refr}}}{T_{\text{evap}}^{\text{refr}}} + \frac{T_{\text{cond}}^{\text{refr}} \Delta S_{\text{intermal}}}{Q_{\text{evap}}} + \frac{Q_{\text{evap}}^{\text{leak}}}{Q_{\text{evap}}} \left( \frac{T_{\text{cond}}^{\text{refr}}}{T_{\text{evap}}^{\text{refr}}} - 1 \right) + \frac{Q_{\text{evap}}^{\text{leak}}}{Q_{\text{evap}}} \quad (\text{A.9})$$

The  $Q^{\text{leak}}$  terms in equation (A.9) can be further combined to yield:

$$\frac{1}{\text{COP}} = -1 + \frac{T_{\text{cond}}^{\text{refr}}}{T_{\text{evap}}^{\text{refr}}} + \frac{T_{\text{cond}}^{\text{refr}} \Delta S_{\text{intermal}}}{Q_{\text{evap}}} + \frac{1}{Q_{\text{evap}}} \left[ Q_{\text{evap}}^{\text{leak}} \left( \frac{T_{\text{cond}}^{\text{refr}}}{T_{\text{evap}}^{\text{refr}}} - 1 \right) + Q_{\text{comp}}^{\text{leak}} \right] \quad (\text{A.10})$$

The  $Q^{\text{leak}}$  terms in equation (A.10) are multiplied by unity in the form of  $\frac{T_{\text{cond}}}{T_{\text{cond}}}$

to obtain:

$$\frac{1}{\text{COP}} = -1 + \frac{T_{\text{cond}}^{\text{refr}}}{T_{\text{evap}}^{\text{refr}}} + \frac{T_{\text{cond}}^{\text{refr}} \Delta S_{\text{intermal}}}{Q_{\text{evap}}} + \frac{T_{\text{cond}}^{\text{refr}}}{Q_{\text{evap}}} \left[ \frac{Q_{\text{evap}}^{\text{leak}}}{T_{\text{cond}}^{\text{refr}}} \left( \frac{T_{\text{cond}}^{\text{refr}}}{T_{\text{evap}}^{\text{refr}}} - 1 \right) + \frac{Q_{\text{comp}}^{\text{leak}}}{T_{\text{cond}}^{\text{refr}}} \right] \quad (\text{A.11})$$

The terms inside the brackets of equation (A.11) are rearranged to give:

$$\frac{1}{\text{COP}} = -1 + \frac{T_{\text{cond}}^{\text{refr}}}{T_{\text{evap}}^{\text{refr}}} + \frac{T_{\text{cond}}^{\text{refr}} \Delta S_{\text{internal}}}{Q_{\text{evap}}} + \frac{T_{\text{cond}}^{\text{refr}}}{Q_{\text{evap}}} \left[ \frac{Q_{\text{comp}}^{\text{leak}}}{T_{\text{cond}}^{\text{refr}}} + Q_{\text{evap}}^{\text{leak}} \left( \frac{1}{T_{\text{evap}}^{\text{refr}}} - \frac{1}{T_{\text{cond}}^{\text{refr}}} \right) \right] \quad (\text{A.12})$$

The  $Q^{\text{leak}}$  terms in the brackets of equation (A.12) can then be described in terms of an entropy production term due to heat leaks. This entropy production term,  $\Delta S_{\text{leak}}$ , is defined to be:

$$\Delta S_{\text{leak}} = \frac{Q_{\text{comp}}^{\text{leak}}}{T_{\text{cond}}^{\text{refr}}} + Q_{\text{evap}}^{\text{leak}} \left( \frac{1}{T_{\text{evap}}^{\text{refr}}} - \frac{1}{T_{\text{cond}}^{\text{refr}}} \right) \quad (\text{A.13})$$

Inserting equation (A.13) into equation (A.12) gives a simplified thermodynamic equation that governs chiller performance:

$$\frac{1}{\text{COP}} = -1 + \frac{T_{\text{cond}}^{\text{refr}}}{T_{\text{evap}}^{\text{refr}}} + \frac{T_{\text{cond}}^{\text{refr}} \Delta S_{\text{internal}}}{Q_{\text{evap}}} + \frac{T_{\text{cond}}^{\text{refr}} \Delta S_{\text{leak}}}{Q_{\text{evap}}} \quad (\text{A.14})$$

The temperatures in these equations are refrigerant temperatures. Refrigerant temperatures are not usually measured in a chiller plant. However, the temperatures of the fluid being cooled and the temperature condenser coolant are often measured. In order to relate equation (A.14) with the measured temperatures, the heat transfer equations at the condenser and evaporator are utilized.

$$Q_{\text{cond}} = (\dot{m} c_p \varepsilon)_{\text{cond}} (T_{\text{cond}}^{\text{refr}} - T_{\text{cond}}^{\text{w\_in}}) \quad (\text{A.15})$$

$$Q_{\text{evap}} = (\dot{m} c_p \varepsilon)_{\text{evap}} (T_{\text{evap}}^{\text{w\_in}} - T_{\text{evap}}^{\text{refr}}) \quad (\text{A.16})$$

where

$\dot{m}$  = coolant (water) mass flow rate, lb/min,

$c_p$  = coolant (water) specific heat, Btu/lb\*R,

$\varepsilon$  = heat exchanger effectiveness,

$T_{\text{cond}}^{\text{w\_in}}$  = condenser entering coolant (water) temperature, R,

$T_{\text{evap}}^{\text{w\_in}}$  = evaporator entering coolant (water) temperature, R.



Solving equations (A.15) and (A.16) for the refrigerant temperatures gives:

$$T_{\text{cond}}^{\text{refr}} = \frac{Q_{\text{cond}}}{\left(\frac{\dot{m} c_p \varepsilon}{\text{cond}}\right)} + T_{\text{cond}}^{\text{w\_in}} \quad (\text{A.17})$$

$$T_{\text{evap}}^{\text{refr}} = T_{\text{evap}}^{\text{w\_in}} - \frac{Q_{\text{evap}}}{\left(\frac{\dot{m} c_p \varepsilon}{\text{evap}}\right)} \quad (\text{A.18})$$

Inserting equations (A.17) and (A.18) into equation (A.14) gives the following:

$$\frac{1}{\text{COP}} = -1 + \frac{\frac{Q_{\text{cond}}}{\left(\frac{\dot{m} c_p \varepsilon}{\text{cond}}\right)} + T_{\text{cond}}^{\text{w\_in}}}{T_{\text{evap}}^{\text{w\_in}} - \frac{Q_{\text{evap}}}{\left(\frac{\dot{m} c_p \varepsilon}{\text{evap}}\right)}} + \frac{\left(\frac{Q_{\text{cond}}}{\left(\frac{\dot{m} c_p \varepsilon}{\text{cond}}\right)} + T_{\text{cond}}^{\text{w\_in}}\right) \Delta S_{\text{int ernal}}}{Q_{\text{evap}}} + \frac{\left(\frac{Q_{\text{cond}}}{\left(\frac{\dot{m} c_p \varepsilon}{\text{cond}}\right)} + T_{\text{cond}}^{\text{w\_in}}\right) \Delta S_{\text{leak}}}{Q_{\text{evap}}} \quad (\text{A.19})$$

The  $Q_{\text{cond}}$  term reappears in equation (A.19). Gordon and Chua insert equation (A.3) into equation (A.19) to eliminate the  $Q_{\text{cond}}$  term. However, this results in  $Q_{\text{cond}}$  terms of higher order which are then neglected. If the condenser coolant entering and leaving temperatures are known,  $Q_{\text{cond}}$  can be expressed as follows

$$Q_{\text{cond}} = (\dot{m} c_p)_{\text{cond}} (T_{\text{cond}}^{\text{w-out}} - T_{\text{cond}}^{\text{w-in}}) \quad (\text{A.20})$$

where

$\dot{m}$  = coolant (water) mass flow rate, lb/min,

$c_p$  = coolant (water) specific heat, Btu/lb\*R,

$T_{\text{cond}}^{\text{w-out}}$  = condenser leaving water temperature, R,

$T_{\text{cond}}^{\text{w-in}}$  = condenser entering water temperature, R.

In the same way,  $Q_{\text{evap}}$  can be expressed as

$$Q_{\text{evap}} = (\dot{m}c_p)_{\text{evap}} (T_{\text{evap}}^{\text{w\_in}} - T_{\text{evap}}^{\text{w\_out}}) \quad (\text{A.21})$$

where

$\dot{m}$  = coolant (water) mass flow rate, lb/min,

$c_p$  = coolant (water) specific heat, Btu/lb\*R,

$T_{\text{evap}}^{\text{w\_out}}$  = evaporator leaving water temperature, R,

$T_{\text{evap}}^{\text{w\_in}}$  = evaporator entering water temperature, R .

Inserting equations (A.20) and (A.21) into equation (A.19) gives:

$$\begin{aligned} \frac{1}{\text{COP}} = & -1 + \frac{\frac{(\dot{m}c_p)_{\text{cond}} (T_{\text{cond}}^{\text{w\_out}} - T_{\text{cond}}^{\text{w\_in}})}{(\dot{m}c_p \varepsilon)_{\text{cond}}} + T_{\text{cond}}^{\text{w\_in}}}{T_{\text{evap}}^{\text{w\_in}} - \frac{(\dot{m}c_p)_{\text{evap}} (T_{\text{evap}}^{\text{w\_in}} - T_{\text{evap}}^{\text{w\_out}})}{(\dot{m}c_p \varepsilon)_{\text{evap}}}} \\ & + \frac{\left( \frac{(\dot{m}c_p)_{\text{cond}} (T_{\text{cond}}^{\text{w\_out}} - T_{\text{cond}}^{\text{w\_in}})}{(\dot{m}c_p \varepsilon)_{\text{cond}}} + T_{\text{cond}}^{\text{w\_in}} \right) \Delta S_{\text{internal}}}{(\dot{m}c_p)_{\text{evap}} (T_{\text{evap}}^{\text{w\_in}} - T_{\text{evap}}^{\text{w\_out}})} \\ & + \frac{\left( \frac{(\dot{m}c_p)_{\text{cond}} (T_{\text{cond}}^{\text{w\_out}} - T_{\text{cond}}^{\text{w\_in}})}{(\dot{m}c_p \varepsilon)_{\text{cond}}} + T_{\text{cond}}^{\text{w\_in}} \right) \Delta S_{\text{leak}}}{(\dot{m}c_p)_{\text{evap}} (T_{\text{evap}}^{\text{w\_in}} - T_{\text{evap}}^{\text{w\_out}})} \end{aligned} \quad (\text{A.22})$$

Simplifying the equation (A.22) by dividing out the common mass flow rates and specific heats yields:

$$\begin{aligned}
 \frac{1}{\text{COP}} = & -1 + \frac{\left( \frac{T_{\text{cond}}^{\text{w\_out}} - T_{\text{condenser}}^{\text{w\_in}}}{\epsilon_{\text{cond}}} + T_{\text{cond}}^{\text{w\_in}} \right)}{T_{\text{evap}}^{\text{w\_in}} - \frac{\left( T_{\text{evap}}^{\text{w\_in}} - T_{\text{evap}}^{\text{w\_out}} \right)}{\epsilon_{\text{evap}}}} \\
 & + \frac{\left( \frac{T_{\text{cond}}^{\text{w\_out}} - T_{\text{cond}}^{\text{w\_in}}}{\epsilon_{\text{cond}}} + T_{\text{cond}}^{\text{w\_in}} \right) \Delta S_{\text{internal}}}{\left( \dot{m} c_p \right)_{\text{evap}} \left( T_{\text{evap}}^{\text{w\_in}} - T_{\text{evap}}^{\text{w\_out}} \right)} \\
 & + \frac{\left( \frac{T_{\text{cond}}^{\text{w\_out}} - T_{\text{cond}}^{\text{w\_in}}}{\epsilon_{\text{cond}}} + T_{\text{cond}}^{\text{w\_in}} \right) \Delta S_{\text{leak}}}{\left( \dot{m} c_p \right)_{\text{evap}} \left( T_{\text{evap}}^{\text{w\_in}} - T_{\text{evap}}^{\text{w\_out}} \right)}
 \end{aligned} \tag{A.23}$$

Equation (A.23) can be used to determine the COP of a chiller using only the chiller coolant temperatures, effectiveness of each heat exchanger, entropy changes, and the mass flow of coolant through the evaporator.

The equation for the compressor input power can be obtained by multiplying both sides of equation (A.23) by  $Q_{\text{evap}}$ , giving:

$$\begin{aligned}
 P_{\text{in}} = & -Q_{\text{evap}} + \frac{Q_{\text{evap}} \left( \frac{T_{\text{cond}}^{\text{w\_out}} - T_{\text{cond}}^{\text{w\_in}}}{\epsilon_{\text{cond}}} + T_{\text{cond}}^{\text{w\_in}} \right)}{T_{\text{evap}}^{\text{w\_in}} - \frac{(T_{\text{evap}}^{\text{w\_in}} - T_{\text{evap}}^{\text{w\_out}})}{\epsilon_{\text{evap}}}} \\
 & + \frac{Q_{\text{evap}} \left( \frac{T_{\text{cond}}^{\text{w\_out}} - T_{\text{cond}}^{\text{w\_in}}}{\epsilon_{\text{cond}}} + T_{\text{cond}}^{\text{w\_in}} \right) \Delta S_{\text{internal}}}{(\dot{m}c_p)_{\text{evap}} (T_{\text{evap}}^{\text{w\_in}} - T_{\text{evap}}^{\text{w\_out}})} \\
 & + \frac{Q_{\text{evap}} \left( \frac{T_{\text{cond}}^{\text{w\_out}} - T_{\text{cond}}^{\text{w\_in}}}{\epsilon_{\text{cond}}} + T_{\text{cond}}^{\text{w\_in}} \right) \Delta S_{\text{leak}}}{(\dot{m}c_p)_{\text{evap}} (T_{\text{evap}}^{\text{w\_in}} - T_{\text{evap}}^{\text{w\_out}})}
 \end{aligned} \tag{A.24}$$

By inserting equation (A.21) into equation (A.24) gives the following:

$$\begin{aligned}
 P_{\text{in}} = & -(\dot{m}c_p)_{\text{evap}} (T_{\text{evap}}^{\text{w\_in}} - T_{\text{evap}}^{\text{w\_out}}) \\
 & + \frac{(\dot{m}c_p)_{\text{evap}} (T_{\text{evap}}^{\text{w\_in}} - T_{\text{evap}}^{\text{w\_out}}) \left( \frac{(T_{\text{cond}}^{\text{w\_out}} - T_{\text{cond}}^{\text{w\_in}})}{\epsilon_{\text{cond}}} + T_{\text{cond}}^{\text{w\_in}} \right)}{T_{\text{evap}}^{\text{w\_in}} - \frac{(T_{\text{evap}}^{\text{w\_in}} - T_{\text{evap}}^{\text{w\_out}})}{\epsilon_{\text{evap}}}} \\
 & + \frac{(\dot{m}c_p)_{\text{evap}} (T_{\text{evap}}^{\text{w\_in}} - T_{\text{evap}}^{\text{w\_out}}) \left( \frac{T_{\text{cond}}^{\text{w\_out}} - T_{\text{cond}}^{\text{w\_in}}}{\epsilon_{\text{cond}}} + T_{\text{cond}}^{\text{w\_in}} \right) \Delta S_{\text{internal}}}{(\dot{m}c_p)_{\text{evap}} (T_{\text{evap}}^{\text{w\_in}} - T_{\text{evap}}^{\text{w\_out}})} \\
 & + \frac{(\dot{m}c_p)_{\text{evap}} (T_{\text{evap}}^{\text{w\_in}} - T_{\text{evap}}^{\text{w\_out}}) \left( \frac{T_{\text{cond}}^{\text{w\_out}} - T_{\text{cond}}^{\text{w\_in}}}{\epsilon_{\text{cond}}} + T_{\text{cond}}^{\text{w\_in}} \right) \Delta S_{\text{leak}}}{(\dot{m}c_p)_{\text{evap}} (T_{\text{evap}}^{\text{w\_in}} - T_{\text{evap}}^{\text{w\_out}})}
 \end{aligned} \tag{A.25}$$

Dividing out the common terms on the right-hand side of equation (A.25) yields:

$$\begin{aligned}
 P_{in} = & -\left(\frac{\dot{m}}{\rho}\right)_{evap} \left(T_{evap}^{w\_in} - T_{evap}^{w\_out}\right) \\
 & + \frac{\left(\frac{\dot{m}}{\rho}\right)_{evap} \left(T_{evap}^{w\_in} - T_{evap}^{w\_out}\right) \left(\frac{T_{cond}^{w\_out} - T_{cond}^{w\_in}}{\epsilon_{cond}} + T_{cond}^{w\_in}\right)}{T_{evap}^{w\_in} - \frac{\left(T_{evap}^{w\_in} - T_{evap}^{w\_out}\right)}{\epsilon_{evap}}} \\
 & + \left(\frac{T_{cond}^{w\_out} - T_{cond}^{w\_in}}{\epsilon_{cond}} + T_{cond}^{w\_in}\right) \Delta S_{internal} \\
 & + \left(\frac{T_{cond}^{w\_out} - T_{cond}^{w\_in}}{\epsilon_{cond}} + T_{cond}^{w\_in}\right) \Delta S_{leak}
 \end{aligned} \tag{A.26}$$

Equation (A.26) is an expression for  $P_{in}$  in terms of the chiller coolant temperatures, effectiveness of each heat exchanger, entropy changes, and the mass flow of coolant through the evaporator.

If both the refrigerant and coolant temperatures are measured, then equation (A.21) can be substituted directly into equation (A.14) to give the following:

$$\frac{1}{COP} = -1 + \frac{T_{cond}^{refr}}{T_{evap}^{refr}} + \frac{T_{cond}^{refr} \Delta S_{internal}}{\left(\frac{\dot{m}}{\rho}\right)_{evap} \left(T_{evap}^{w\_in} - T_{evap}^{w\_out}\right)} + \frac{T_{cond}^{refr} \Delta S_{leak}}{\left(\frac{\dot{m}}{\rho}\right)_{evap} \left(T_{evap}^{w\_in} - T_{evap}^{w\_out}\right)} \tag{A.27}$$

Equation (A.27) can be used to determine the COP of a chiller using only the chiller coolant temperatures, refrigerant temperatures, entropy changes, and the mass flow of coolant through the evaporator. The equation for the compressor input power can be obtained by multiplying both sides of equation (A.14) by  $Q_{\text{evap}}$ , giving:

$$P_{\text{in}} = -Q_{\text{evap}} + \frac{Q_{\text{evap}} T_{\text{cond}}^{\text{refr}}}{T_{\text{evap}}^{\text{refr}}} + T_{\text{cond}}^{\text{refr}} \Delta S_{\text{internal}} + T_{\text{cond}}^{\text{refr}} \Delta S_{\text{leak}} \quad (\text{A.28})$$

Inserting equation (A.21) into equation (A.23) gives:

$$P_{\text{in}} = -(\dot{m} c_p)_{\text{evap}} (T_{\text{evap}}^{\text{w\_in}} - T_{\text{evap}}^{\text{w\_out}}) + \frac{(\dot{m} c_p)_{\text{evap}} (T_{\text{evap}}^{\text{w\_in}} - T_{\text{evap}}^{\text{w\_out}}) T_{\text{cond}}^{\text{refr}}}{T_{\text{evap}}^{\text{refr}}} + T_{\text{cond}}^{\text{refr}} \Delta S_{\text{internal}} + T_{\text{cond}}^{\text{refr}} \Delta S_{\text{leak}} \quad (\text{A.29})$$

Equation (A.29) is an expression for  $P_{\text{in}}$  in terms of the chiller coolant temperatures, refrigerant temperatures, entropy changes, and the mass flow of coolant through the evaporator. Combining the  $\Delta S$  terms in equation (A.29) gives:

$$P_{\text{in}} = -(\dot{m} c_p)_{\text{evap}} (T_{\text{evap}}^{\text{w\_in}} - T_{\text{evap}}^{\text{w\_out}}) + \frac{(\dot{m} c_p)_{\text{evap}} (T_{\text{evap}}^{\text{w\_in}} - T_{\text{evap}}^{\text{w\_out}}) T_{\text{cond}}^{\text{refr}}}{T_{\text{evap}}^{\text{refr}}} + T_{\text{cond}}^{\text{refr}} \Delta S_{\text{total}} \quad (\text{A.30})$$

Solving equation (A.30) for  $\Delta S_{\text{total}}$  yields:

$$\Delta S_{\text{total}} = \frac{P_{\text{in}}}{T_{\text{cond}}^{\text{refr}}} + \frac{\left(\frac{m}{p}\right)_{\text{evap}} (T_{\text{evap}}^{\text{w-in}} - T_{\text{evap}}^{\text{w-out}})}{T_{\text{cond}}^{\text{refr}}} - \frac{\left(\frac{m}{p}\right)_{\text{evap}} (T_{\text{evap}}^{\text{w-in}} - T_{\text{evap}}^{\text{w-out}})}{T_{\text{evap}}^{\text{refr}}} \quad (\text{A.31})$$

Equation (A.31) is used to calculate the change in entropy using the evaporator measurements. A multiple linear regression of the change in entropy versus the difference in refrigerant temperatures and the change in water temperature across the evaporator provides:

$$\Delta S_{\text{total}} = -0.0001608(T_{\text{cond}}^{\text{refr}} - T_{\text{evap}}^{\text{refr}}) - 0.00176(T_{\text{evap}}^{\text{w-in}} - T_{\text{evap}}^{\text{w-out}}) + 0.05605 \quad (\text{A.32})$$

Inserting equation (A.32) into equation (A.30) gives:

$$P_{\text{in}} = -\left(\frac{m}{p}\right)_{\text{evap}} (T_{\text{evap}}^{\text{w-in}} - T_{\text{evap}}^{\text{w-out}}) + \frac{\left(\frac{m}{p}\right)_{\text{evap}} (T_{\text{evap}}^{\text{w-in}} - T_{\text{evap}}^{\text{w-out}}) T_{\text{cond}}^{\text{refr}}}{T_{\text{evap}}^{\text{refr}}} + T_{\text{cond}}^{\text{refr}} \left[ -0.0001608(T_{\text{cond}}^{\text{refr}} - T_{\text{evap}}^{\text{refr}}) - 0.00176(T_{\text{evap}}^{\text{w-in}} - T_{\text{evap}}^{\text{w-out}}) + 0.05605 \right] \quad (\text{A.33})$$



Equation (A.33) allows the computation of chiller power using the evaporator coolant temperatures, refrigerant temperatures, pressure change across the compressor, and the mass flow of coolant through the evaporator. In addition to the compressor power, the condenser pressure and condenser leaving water temperature are desired variables for calculation. The calculation of the condenser pressure will ensure that the condenser pressures do not exceed the capability of the chiller. The calculation of the condenser leaving water temperature will be used in the cooling tower model to re-evaluate the condenser entering water temperature. In order to calculate these values, the chiller power input must be defined in terms of condenser variables. Returning to the 1<sup>st</sup> and 2<sup>nd</sup> Law and solving equation (A.2) for  $Q_{\text{evap}}$  gives the following:

$$Q_{\text{evap}} = \frac{T_{\text{evap}}^{\text{refr}}}{T_{\text{cond}}^{\text{refr}}} (Q_{\text{cond}} + Q_{\text{cond}}^{\text{leak}}) - T_{\text{evap}}^{\text{refr}} \Delta S_{\text{internal}} - Q_{\text{evap}}^{\text{leak}} \quad (\text{A.34})$$

Inserting  $Q_{\text{evap}}$  obtained in equation (A.34) into equation (A.1) yields:

$$0 = Q_{\text{cond}} + Q_{\text{cond}}^{\text{leak}} - \frac{T_{\text{evap}}^{\text{refr}}}{T_{\text{cond}}^{\text{refr}}} (Q_{\text{cond}} + Q_{\text{cond}}^{\text{leak}}) + T_{\text{evap}}^{\text{refr}} \Delta S_{\text{internal}} + Q_{\text{evap}}^{\text{leak}} - Q_{\text{evap}}^{\text{leak}} - P_{\text{in}} + Q_{\text{comp}}^{\text{leak}} \quad (\text{A.35})$$

The  $Q_{\text{evap}}^{\text{leak}}$  term cancels out and equation (A.35) is solved for  $P_{\text{in}}$  to obtain:

$$P_{\text{in}} = Q_{\text{cond}} + Q_{\text{cond}}^{\text{leak}} - \frac{T_{\text{evap}}^{\text{refr}}}{T_{\text{cond}}^{\text{refr}}} (Q_{\text{cond}} + Q_{\text{cond}}^{\text{leak}}) + T_{\text{evap}}^{\text{refr}} \Delta S_{\text{int ernal}} + Q_{\text{compressor}}^{\text{leak}} \quad (\text{A.36})$$

By combining the  $Q_{\text{evap}}$  and  $Q_{\text{evap}}^{\text{leak}}$  terms, equation (A.36) becomes:

$$P_{\text{in}} = Q_{\text{cond}} \left( 1 - \frac{T_{\text{evap}}^{\text{refr}}}{T_{\text{cond}}^{\text{refr}}} \right) + Q_{\text{cond}}^{\text{leak}} \left( 1 - \frac{T_{\text{evap}}^{\text{refr}}}{T_{\text{cond}}^{\text{refr}}} \right) + Q_{\text{comp}}^{\text{leak}} + T_{\text{evap}}^{\text{refr}} \Delta S_{\text{int ernal}} \quad (\text{A.37})$$

Dividing both sides of equation (A.37) by  $Q_{\text{cond}}$  gives:

$$\frac{P_{\text{in}}}{Q_{\text{cond}}} = 1 - \frac{T_{\text{evap}}^{\text{refr}}}{T_{\text{cond}}^{\text{refr}}} + \frac{Q_{\text{cond}}^{\text{leak}}}{Q_{\text{cond}}} \left( 1 - \frac{T_{\text{evap}}^{\text{refr}}}{T_{\text{cond}}^{\text{refr}}} \right) + \frac{Q_{\text{comp}}^{\text{leak}}}{Q_{\text{cond}}} + \frac{T_{\text{evap}}^{\text{refr}} \Delta S_{\text{int ernal}}}{Q_{\text{cond}}} \quad (\text{A.38})$$

Moving the  $Q^{\text{leak}}$  terms to the end of the equation (A.38) gives:

$$\frac{P_{\text{in}}}{Q_{\text{cond}}} = 1 - \frac{T_{\text{evap}}^{\text{refr}}}{T_{\text{cond}}^{\text{refr}}} + \frac{T_{\text{evap}}^{\text{refr}} \Delta S_{\text{int ernal}}}{Q_{\text{cond}}} + \frac{Q_{\text{cond}}^{\text{leak}}}{Q_{\text{cond}}} \left( 1 - \frac{T_{\text{evap}}^{\text{refr}}}{T_{\text{cond}}^{\text{refr}}} \right) + \frac{Q_{\text{comp}}^{\text{leak}}}{Q_{\text{cond}}} \quad (\text{A.39})$$

The  $Q^{\text{leak}}$  terms in equation (A.39) can be further combined to yield:

$$\frac{P_{\text{in}}}{Q_{\text{cond}}} = 1 - \frac{T_{\text{evap}}^{\text{refr}}}{T_{\text{cond}}^{\text{refr}}} + \frac{T_{\text{evap}}^{\text{refr}} \Delta S_{\text{internal}}}{Q_{\text{cond}}} + \frac{1}{Q_{\text{cond}}} \left[ Q_{\text{cond}}^{\text{leak}} \left( 1 - \frac{T_{\text{evap}}^{\text{refr}}}{T_{\text{cond}}^{\text{refr}}} \right) + Q_{\text{comp}}^{\text{leak}} \right] \quad (\text{A.40})$$

The  $Q^{\text{leak}}$  terms in equation (A.40) are multiplied by unity in the form of  $\frac{T_{\text{evap}}}{T_{\text{evap}}}$  to

obtain:

$$\frac{P_{\text{in}}}{Q_{\text{cond}}} = 1 - \frac{T_{\text{evap}}^{\text{refr}}}{T_{\text{cond}}^{\text{refr}}} + \frac{T_{\text{evap}}^{\text{refr}} \Delta S_{\text{internal}}}{Q_{\text{cond}}} + \frac{T_{\text{evap}}^{\text{refr}}}{Q_{\text{cond}}} \left[ \frac{Q_{\text{cond}}^{\text{leak}}}{T_{\text{evap}}^{\text{refr}}} \left( 1 - \frac{T_{\text{evap}}^{\text{refr}}}{T_{\text{cond}}^{\text{refr}}} \right) + \frac{Q_{\text{comp}}^{\text{leak}}}{T_{\text{evap}}^{\text{refr}}} \right] \quad (\text{A.41})$$

The terms inside the brackets of equation (A.41) are rearranged to give:

$$\frac{P_{\text{in}}}{Q_{\text{cond}}} = 1 - \frac{T_{\text{evap}}^{\text{refr}}}{T_{\text{cond}}^{\text{refr}}} + \frac{T_{\text{evap}}^{\text{refr}} \Delta S_{\text{internal}}}{Q_{\text{cond}}} + \frac{T_{\text{evap}}^{\text{refr}}}{Q_{\text{cond}}} \left[ \frac{Q_{\text{comp}}^{\text{leak}}}{T_{\text{evap}}^{\text{refr}}} + Q_{\text{cond}}^{\text{leak}} \left( \frac{1}{T_{\text{evap}}^{\text{refr}}} - \frac{1}{T_{\text{cond}}^{\text{refr}}} \right) \right] \quad (\text{A.42})$$

The  $Q^{\text{leak}}$  terms in the brackets of equation (A.42) can then be described in terms of an entropy production term due to heat leaks. This entropy production term,  $\Delta S_{\text{leak}}$ , is defined to be:

$$\Delta S_{\text{leak}} = \frac{Q_{\text{comp}}^{\text{leak}}}{T_{\text{evap}}^{\text{refr}}} + Q_{\text{cond}}^{\text{leak}} \left( \frac{1}{T_{\text{evap}}^{\text{refr}}} - \frac{1}{T_{\text{cond}}^{\text{refr}}} \right) \quad (\text{A.43})$$

Inserting equation (A.43) into equation (A.42) gives:

$$\frac{P_{\text{in}}}{Q_{\text{cond}}} = 1 - \frac{T_{\text{evap}}^{\text{refr}}}{T_{\text{cond}}^{\text{refr}}} + \frac{T_{\text{evap}}^{\text{refr}} \Delta S_{\text{internal}}}{Q_{\text{cond}}} + \frac{T_{\text{evap}}^{\text{refr}} \Delta S_{\text{leak}}}{Q_{\text{cond}}} \quad (\text{A.44})$$

Solving equation (A.44) for  $P_{\text{in}}$  gives a simplified equation that will govern chiller performance:

$$P_{\text{in}} = Q_{\text{cond}} - \frac{T_{\text{evap}}^{\text{refr}} Q_{\text{condenser}}}{T_{\text{cond}}^{\text{refr}}} + T_{\text{evap}}^{\text{refr}} \Delta S_{\text{internal}} + T_{\text{evap}}^{\text{refr}} \Delta S_{\text{leak}} \quad (\text{A.45})$$

The temperatures in these equations are refrigerant temperatures. Refrigerant temperatures are not usually measured in a chiller plant. However, the temperatures of

the fluid being cooled and the temperature condenser coolant are often measured. In order to relate equation (A.45) with the measured temperatures, the heat transfer equations at the condenser and evaporator are utilized.

$$Q_{\text{cond}} = (\dot{m} c_p \varepsilon)_{\text{cond}} (T_{\text{cond}}^{\text{refr}} - T_{\text{cond}}^{\text{w\_in}}) \quad (\text{A.46})$$

$$Q_{\text{evap}} = (\dot{m} c_p \varepsilon)_{\text{evap}} (T_{\text{evap}}^{\text{w\_in}} - T_{\text{evap}}^{\text{refr}}) \quad (\text{A.47})$$

where

$\dot{m}$  = coolant (water) mass flow rate, lb/min,

$c_p$  = coolant (water) specific heat, Btu/lb\*R,

$\varepsilon$  = heat exchanger effectiveness,

$T_{\text{cond}}^{\text{w\_in}}$  = condenser entering coolant (water) temperature, R,

$T_{\text{evap}}^{\text{w\_in}}$  = evaporator entering coolant (water) temperature, R.

Solving equations (A.46) and (A.47) for the refrigerant temperatures gives:

$$T_{\text{cond}}^{\text{refr}} = \frac{Q_{\text{cond}}}{\left(\frac{\dot{m} c_p \varepsilon}{\text{cond}}\right)} + T_{\text{cond}}^{\text{w\_in}} \quad (\text{A.48})$$

$$T_{\text{evap}}^{\text{refr}} = T_{\text{evap}}^{\text{w\_in}} - \frac{Q_{\text{evap}}}{\left(\frac{\dot{m} c_p \varepsilon}{\text{evap}}\right)} \quad (\text{A.49})$$

Inserting equations (A.48) and (A.49) into equation (A.45) gives the following:

$$\begin{aligned} P_{\text{in}} = & Q_{\text{cond}} - \frac{\left( T_{\text{evap}}^{\text{w\_in}} - \frac{Q_{\text{evap}}}{\left(\frac{\dot{m} c_p \varepsilon}{\text{evap}}\right)} \right) Q_{\text{cond}}}{\frac{Q_{\text{cond}}}{\left(\frac{\dot{m} c_p \varepsilon}{\text{cond}}\right)} + T_{\text{cond}}^{\text{w\_in}}} + \left( T_{\text{evap}}^{\text{w\_in}} - \frac{Q_{\text{evap}}}{\left(\frac{\dot{m} c_p \varepsilon}{\text{evap}}\right)} \right) \Delta S_{\text{internal}} \\ & + \left( T_{\text{evap}}^{\text{w\_in}} - \frac{Q_{\text{evap}}}{\left(\frac{\dot{m} c_p \varepsilon}{\text{evap}}\right)} \right) \Delta S_{\text{leak}} \end{aligned} \quad (\text{A.50})$$

The  $Q_{\text{evap}}$  term reappears in equation (A.50). If the evaporator coolant entering and leaving temperatures are known,  $Q_{\text{evap}}$  can be expressed as

$$Q_{\text{evap}} = (\dot{m} c_p)_{\text{evap}} (T_{\text{evap}}^{\text{w-in}} - T_{\text{evap}}^{\text{w-out}}) \quad (\text{A.51})$$

where

$\dot{m}$  = coolant (water) mass flow rate, lb/min,

$c_p$  = coolant (water) specific heat, Btu/lb\*R,

$T_{\text{evap}}^{\text{w-out}}$  = evaporator leaving water temperature, R,

$T_{\text{evap}}^{\text{w-in}}$  = evaporator entering water temperature, R.

In the same way,  $Q_{\text{cond}}$  can be expressed as

$$Q_{\text{cond}} = (\dot{m} c_p)_{\text{cond}} (T_{\text{cond}}^{\text{w-out}} - T_{\text{cond}}^{\text{w-in}}) \quad (\text{A.52})$$

where

$\dot{m}$  = coolant (water) mass flow rate, lb/min,

$c_p$  = coolant (water) specific heat, Btu/lb\*R,

$T_{\text{cond}}^{\text{w-out}}$  = condenser leaving water temperature, R,

$T_{\text{cond}}^{\text{w-in}}$  = condenser entering water temperature, R.

Inserting equations (A.51) and (A.52) into equation (A.50) gives:

$$P_{\text{in}} = \frac{(\dot{m} c_p)_{\text{cond}} (T_{\text{cond}}^{\text{w-out}} - T_{\text{cond}}^{\text{w-in}}) \left( T_{\text{evap}}^{\text{w-in}} - \frac{(\dot{m} c_p)_{\text{evap}} (T_{\text{evap}}^{\text{w-in}} - T_{\text{evap}}^{\text{w-out}})}{(\dot{m} c_p \varepsilon)_{\text{evap}}} \right)}{\frac{(\dot{m} c_p)_{\text{cond}} (T_{\text{cond}}^{\text{w-out}} - T_{\text{cond}}^{\text{w-in}})}{(\dot{m} c_p \varepsilon)_{\text{cond}}} + T_{\text{cond}}^{\text{w-in}}} + \left( T_{\text{evap}}^{\text{w-in}} - \frac{(\dot{m} c_p)_{\text{evap}} (T_{\text{evap}}^{\text{w-in}} - T_{\text{evap}}^{\text{w-out}})}{(\dot{m} c_p \varepsilon)_{\text{evap}}} \right) \Delta S_{\text{internal}} + \left( T_{\text{evap}}^{\text{w-in}} - \frac{(\dot{m} c_p)_{\text{evap}} (T_{\text{evap}}^{\text{w-in}} - T_{\text{evap}}^{\text{w-out}})}{(\dot{m} c_p \varepsilon)_{\text{evap}}} \right) \Delta S_{\text{leak}} \quad (\text{A.53})$$



Simplifying the equation (A.53) by dividing out the common mass flow rates and specific heats yields:

$$\begin{aligned}
 P_{in} = & \left( \dot{m} c_p \right)_{cond} \left( T_{cond}^{w\_out} - T_{cond}^{w\_in} \right) \\
 & \frac{\left( \dot{m} c_p \right)_{cond} \left( T_{cond}^{w\_out} - T_{cond}^{w\_in} \right) \left( T_{evap}^{w\_in} - \frac{\left( T_{evap}^{w\_in} - T_{evap}^{w\_out} \right)}{\epsilon_{evap}} \right)}{T_{cond}^{w\_in} + \frac{\left( T_{cond}^{w\_out} - T_{cond}^{w\_in} \right)}{\epsilon_{cond}}} \\
 & + \left( T_{evap}^{w\_in} - \frac{\left( T_{evap}^{w\_in} - T_{evap}^{w\_out} \right)}{\epsilon_{evap}} \right) \Delta S_{internal} + \left( T_{evap}^{w\_in} - \frac{\left( T_{evap}^{w\_in} - T_{evap}^{w\_out} \right)}{\epsilon_{evap}} \right) \Delta S_{leak}
 \end{aligned} \tag{A.54}$$

Equation (A.54) can be used to determine the compressor power input to a chiller using only the chiller coolant temperatures, effectiveness of each heat exchanger, entropy changes, and the mass flow of coolant through the condenser. If both the refrigerant temperatures and coolant temperatures are measured, then equation (A.52) can be substituted directly into equation (A.45) giving:

$$\begin{aligned}
 P_{in} = & \left( \dot{m} c_p \right)_{cond} \left( T_{cond}^{w\_out} - T_{cond}^{w\_in} \right) - \frac{T_{evap}^{refr} \left( \dot{m} c_p \right)_{cond} \left( T_{cond}^{w\_out} - T_{cond}^{w\_in} \right)}{T_{cond}^{refr}} \\
 & + T_{evap}^{refr} \Delta S_{internal} + T_{evap}^{refr} \Delta S_{leak}
 \end{aligned} \tag{A.55}$$

Combining the  $\Delta S$  terms in equation (A.55) gives:

$$P_{in} = \left(\frac{\dot{m}}{c_p}\right)_{cond} (T_{cond}^{w-out} - T_{cond}^{w-in}) - \frac{T_{evap}^{refr} \left(\frac{\dot{m}}{c_p}\right)_{cond} (T_{cond}^{w-out} - T_{cond}^{w-in})}{T_{cond}^{refr}} + T_{evap}^{refr} \Delta S_{total} \quad (A.56)$$

Solving equation (A.56) for  $\Delta S_{total}$  yields:

$$\Delta S_{total} = \frac{P_{in}}{T_{evap}^{refr}} - \frac{\left(\frac{\dot{m}}{c_p}\right)_{cond} (T_{cond}^{w-out} - T_{cond}^{w-in})}{T_{evap}^{refr}} + \frac{\left(\frac{\dot{m}}{c_p}\right)_{cond} (T_{cond}^{w-out} - T_{cond}^{w-in})}{T_{cond}^{refr}} \quad (A.57)$$

Equation (A.57) is used to calculate the change in entropy using the condenser measurements. A multiple-linear regression of the data provides the empirical correlation between the changes in entropy, refrigerant temperature and evaporator water temperature. This line is described by:

$$\Delta S_{total} = 0.0000666(T_{cond}^{refr} - T_{evap}^{refr}) - 0.00291(T_{cond}^{w-out} - T_{cond}^{w-in}) + 0.05132 \quad (A.58)$$

Inserting equation (A.58) into equation (A.56) gives:

$$P_{in} = \left(\frac{m\dot{c}_p}{\rho}\right)_{\text{condenser}} (T_{\text{cond}}^{\text{w\_out}} - T_{\text{cond}}^{\text{w\_in}}) - \frac{T_{\text{evap}}^{\text{refr}} \left(\frac{m\dot{c}_p}{\rho}\right)_{\text{condenser}} (T_{\text{cond}}^{\text{w\_out}} - T_{\text{cond}}^{\text{w\_in}})}{T_{\text{cond}}^{\text{refr}}} + T_{\text{evap}}^{\text{refr}} \left[ 0.0000666(T_{\text{cond}}^{\text{refr}} - T_{\text{evap}}^{\text{refr}}) - 0.00291(T_{\text{cond}}^{\text{w\_out}} - T_{\text{cond}}^{\text{w\_in}}) + 0.05132 \right] \quad (\text{A.59})$$

Equation (A.59) allows the computation of chiller power using the condenser coolant temperatures, refrigerant temperatures, pressure change across the compressor, and the mass flow of coolant through the condenser. To solve for the condenser coolant leaving temperature, equation (A.45) is first solved for the condenser heat load:

$$P_{in} - T_{\text{evap}}^{\text{refr}} \Delta S_{\text{internal}} - T_{\text{evap}}^{\text{refr}} \Delta S_{\text{leak}} = Q_{\text{cond}} - \frac{T_{\text{evap}}^{\text{refr}} Q_{\text{cond}}}{T_{\text{cond}}^{\text{refr}}} \quad (\text{A.60})$$

Combining the  $\Delta S$  terms and factoring out  $Q_{\text{cond}}$  gives:

$$P_{in} - T_{\text{evap}}^{\text{refr}} \Delta S_{\text{total}} = Q_{\text{cond}} \left( 1 - \frac{T_{\text{evap}}^{\text{refr}}}{T_{\text{cond}}^{\text{refr}}} \right) \quad (\text{A.61})$$

Solving equation (A.61) for  $Q_{\text{cond}}$  yields:

$$Q_{\text{cond}} = \frac{P_{\text{in}} - T_{\text{evap}}^{\text{refr}} \Delta S_{\text{total}}}{\left(1 - \frac{T_{\text{evap}}^{\text{refr}}}{T_{\text{cond}}^{\text{refr}}}\right)} \quad (\text{A.62})$$

Inserting equation (A.52) into equation (A.62) gives:

$$\left(\frac{\dot{m}}{p}\right)_{\text{condenser}} \left(T_{\text{cond}}^{\text{w-out}} - T_{\text{cond}}^{\text{w-in}}\right) = \frac{P_{\text{in}} - T_{\text{evap}}^{\text{refr}} \Delta S_{\text{total}}}{\left(1 - \frac{T_{\text{evap}}^{\text{refr}}}{T_{\text{cond}}^{\text{refr}}}\right)} \quad (\text{A.63})$$

Solving equation (A.63) for  $T_{\text{cond}}^{\text{w-out}}$  obtains:

$$T_{\text{cond}}^{\text{w-out}} = \frac{P_{\text{in}} - T_{\text{evap}}^{\text{refr}} \Delta S_{\text{total}}}{\left(\frac{\dot{m}}{p}\right)_{\text{cond}} \left(1 - \frac{T_{\text{evap}}^{\text{refr}}}{T_{\text{cond}}^{\text{refr}}}\right)} + T_{\text{cond}}^{\text{w-in}} \quad (\text{A.64})$$

Inserting the pressure-entropy correlation described in equation (A.58) yields:

$$T_{\text{cond}}^{\text{w\_out}} = \frac{P_{\text{in}} - T_{\text{evap}}^{\text{refr}} (-0.0009(\Delta P) + 0.0822)}{\left(\frac{d\&C}{dp}\right)_{\text{cond}} \left(1 - \frac{T_{\text{evap}}^{\text{refr}}}{T_{\text{cond}}^{\text{refr}}}\right)} + T_{\text{cond}}^{\text{w\_in}} \quad (\text{A.65})$$

In order to calculate the condenser pressure, it is necessary to calculate the change in pressure across the compressor. This is the  $\Delta P$  term that has been used to calculate the change in entropy in the chiller. Since the evaporation and condensation processes occur at constant pressures and temperatures, there is a strong correlation between the refrigerant condensation and evaporation temperatures and the refrigerant condensation and evaporation pressures, respectively. Consequently, there is a strong correlation between the change in pressure across the compressor and the difference between the condenser and evaporator refrigerant temperatures. A linear regression of this data provides the empirical correlation between the changes in refrigerant temperature and pressure. This line is described by:

$$\Delta T_{\text{refr}} = 0.5902(\Delta P) + 12.338 \quad (\text{A.66})$$

The leaving condenser and leaving evaporator coolant temperatures approach the condenser and evaporator refrigerant temperatures, respectively. Therefore:

$$\Delta T_{\text{refr}} \approx T_{\text{cond}}^{\text{w\_out}} - T_{\text{evap}}^{\text{w\_out}} \quad (\text{A.67})$$

Since  $\Delta T_{\text{refr}}$  is related to  $T_{\text{cond}}^{\text{w\_out}} - T_{\text{evap}}^{\text{w\_out}}$ , there is a relationship between  $T_{\text{cond}}^{\text{w\_out}} - T_{\text{evap}}^{\text{w\_out}}$  and  $\Delta P$ . A linear regression of this data provides the empirical correlation between the changes in refrigerant temperature and pressure. This line is described by:

$$\Delta P = 2.0474(T_{\text{cond}}^{\text{w\_out}} - T_{\text{evap}}^{\text{w\_out}}) - 25.819 \quad (\text{A.68})$$

At this point an iterative solution is employed to calculate the chiller power consumption, the leaving condenser water temperature and the condenser pressure. Guess values for the change in pressure across the compressor and the condenser refrigerant temperature are employed with measured evaporator temperatures and pressures to calculate the compressor power using equation (A.33). This compressor power is then used in equation (A.65) to calculate the condenser coolant leaving temperature. This temperature is used in equation (A.68) to calculate a new value for the

change in pressure across the compressor. Equation (A.66) is employed to calculate the change in refrigerant temperatures. The condenser refrigerant temperature is given by:

$$T_{\text{cond}}^{\text{refr}} = T_{\text{evap}}^{\text{refr}} + \Delta T_{\text{refr}} \quad (\text{A.69})$$

Equation (A.69) is used to calculate a new condenser refrigerant temperature.

The new condenser refrigerant temperature and pressure is used in subsequent iterations.

The model shows convergence after five iterations.

## **APPENDIX B**

### **TEMPERATURE-ENTROPY DIAGRAM EXPLANATION**

In describing the operation of a chiller, the temperature-entropy diagram can be a useful diagnostic tool. To provide an explanation of real chiller operation, the ideal case will be considered and the inefficiencies associated with real operation will be added as the idea is developed. The Carnot Cycle consists of four internally reversible processes and may be used to describe chiller operations. These four processes are an adiabatic compression, isothermal condensation, adiabatic expansion, and isothermal evaporation. These four processes are shown in Figure B.1.



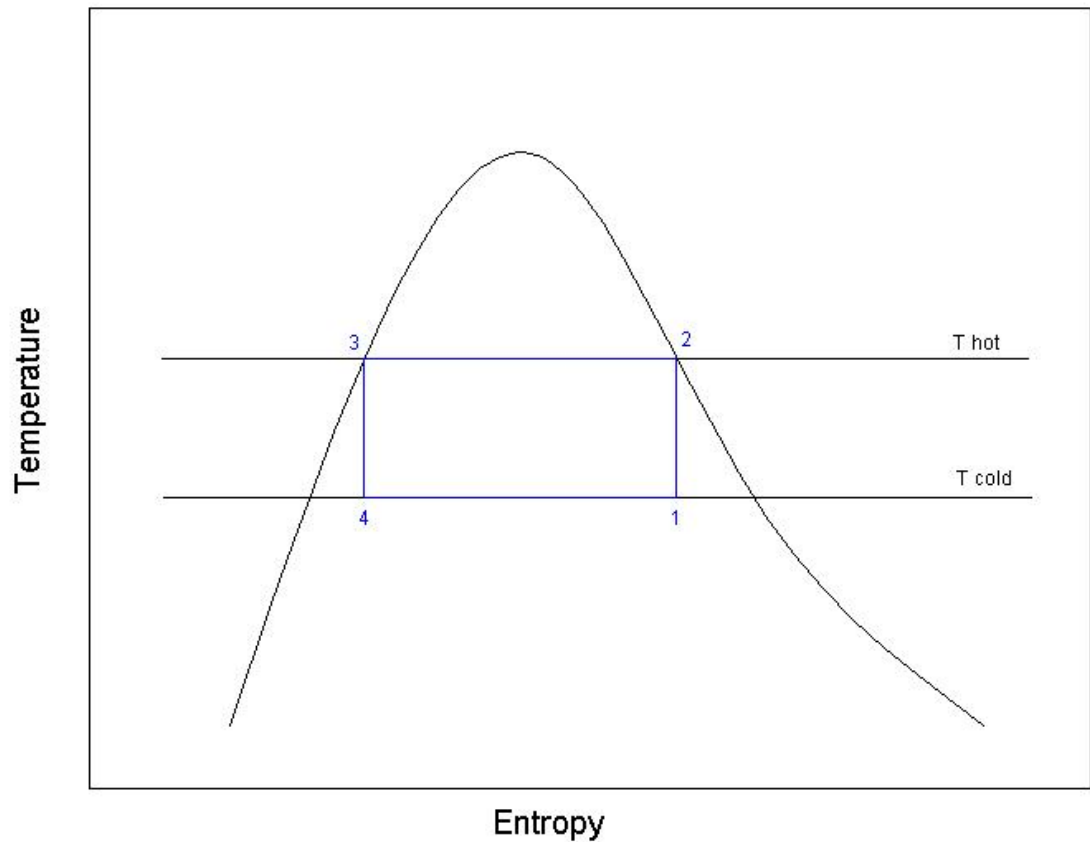


Figure B.1. Ideal Carnot Cycle

The capacity of the chiller is the area under the evaporation line (4-1). The amount of work done by the cycle is the area under the condensation line (2-3) minus the capacity. These definitions for capacity and work will continue to hold true for the other cycles in this investigation.

The first problem encountered with the Carnot Cycle in an explanation of a real refrigeration system is the determination of Point 1. Point 1 exists in the fluid-vapor region of the refrigerant. Point 1 is not distinguishable from the other points along the

Process 4-1 line using readily measured variables such as temperature or pressure. The second problem is that condensation and evaporation take place at the temperature of the hot and cold reservoirs. This would physically mean that no temperature difference exists to drive the heat transfer.

In order to address these problems, the Carnot Cycle is modified to move Point 1 to a measurable condition and to account for the temperature differences between the refrigerant and the reservoirs in the evaporator and condenser. The resulting diagram is shown in Figure B.2.

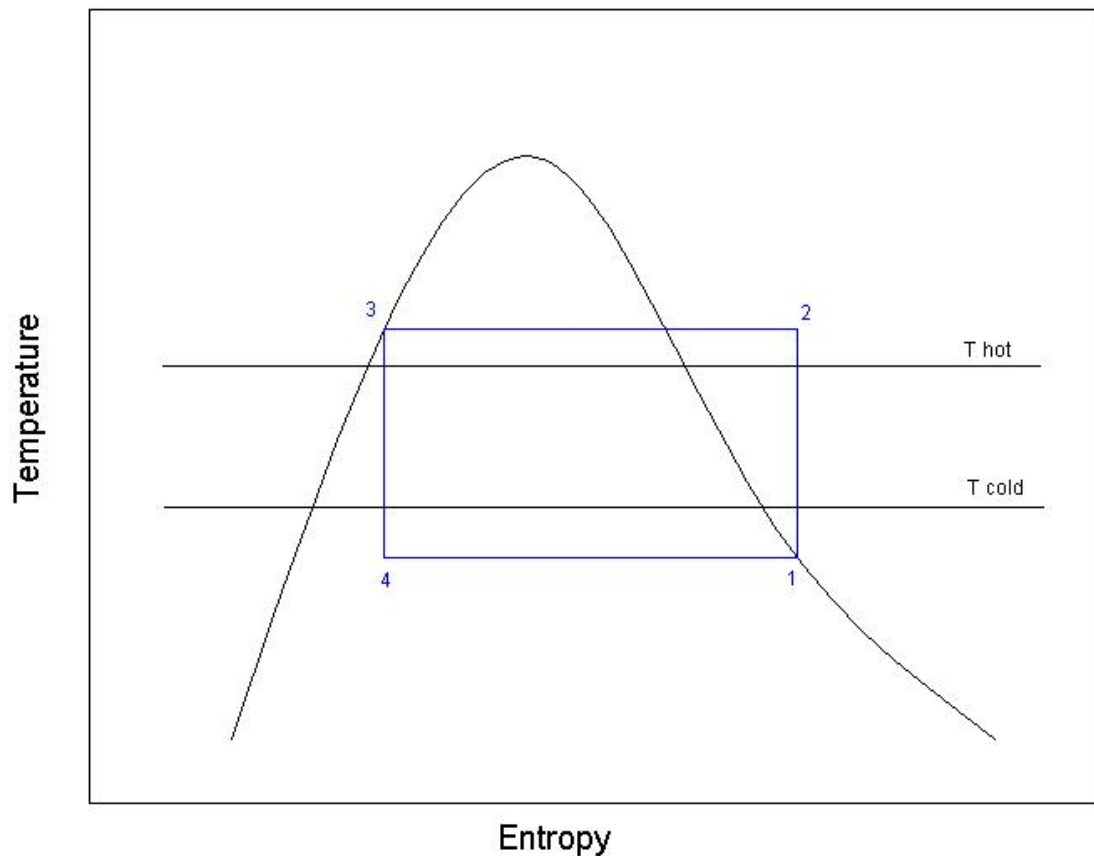


Figure B.2. Modified Carnot Cycle

Point 1 has been moved to the saturated vapor line. This point can be measured using a temperature sensor since the temperature will rise sharply if Point 1 is exceeded. This would indicate that the refrigerant is fully evaporated and has entered a superheated state. The evaporation line has been moved below the cold reservoir temperature while the condensation line has been moved above the hot reservoir temperature. The cold reservoir represents the chilled water temperature and the hot reservoir represents the condenser water temperature. The areas between the reservoir temperatures and the evaporation and condensation lines physically represent the losses due to finite-rate heat transfer in the evaporator and condenser, respectively. Extending Point 1 to the saturated vapor line increases the effective capacity of the chiller with respect to the chiller cycle shown in Figure 1. It should also be noted that the area between the condensation and evaporation lines increased. This physically corresponds to the amount of work required to realize the increased capacity.

The Carnot Cycle shown in Figure B.2 is not without problems. The first problem occurs in moving along the condensation line (2-3). In the superheated vapor region, an isothermal decrease in entropy would correspond to an increase in pressure, i.e. isothermal compression in the condenser. This condition violates the assumption of isentropic compression. A better assumption would be a decrease in temperature and entropy at a constant pressure. The second problem occurs in the assumption of an isentropic expansion. The amount of work that can be obtained by using a turbine in the expansion of the refrigerant is very small for most refrigeration systems. An expansion valve is used in place of the turbine. An isenthalpic expansion is a more realistic

assumption for the expansion process. By modifying the Carnot Cycle to account for these changes, the ideal Rankine Cycle is obtained. The ideal Rankine Cycle is shown in Figure B.3.

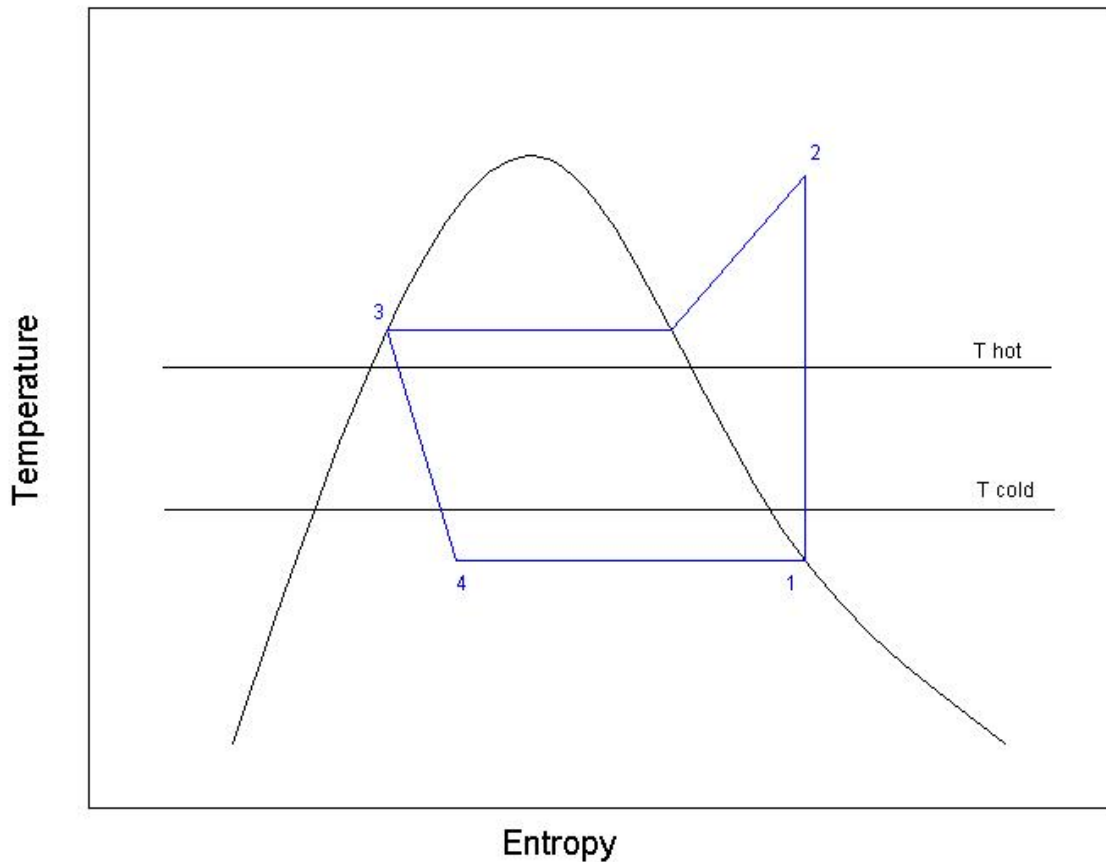


Figure B.3. Rankine Cycle

In the Rankine Cycle, our assumptions have changed significantly. This cycle assumes an isentropic compression, isobaric condensation, isenthalpic expansion, and isothermal evaporation. By using an isenthalpic expansion, the capacity of the Rankine

Cycle decreases in comparison to the capacity of the Carnot Cycle. The combination of an isentropic compression and isobaric condensation results in a superheated refrigerant vapor at the discharge of the compressor. This is graphically represented as the “superheat spike” that is characteristic of the Rankine Cycle. The amount of work required increases since the area under the condensation line now includes the “superheat spike” and the previously mentioned reduction in capacity.

The ideal Rankine Cycle begins to account for work that is done to overcome non-isentropic inefficiencies in the expansion valve. In a real chiller, the compressor behaves in a non-isentropic manner as well. Entropy is produced in the compressor due to frictional losses. In order to ensure that no liquid refrigerant enters the compressor, the refrigerant is allowed to enter the superheated vapor region before compression. Another departure from the ideal Rankine Cycle is the sub-cooling of the refrigerant in the condenser. Accounting for these changes, the diagram in Figure B.4 is obtained.

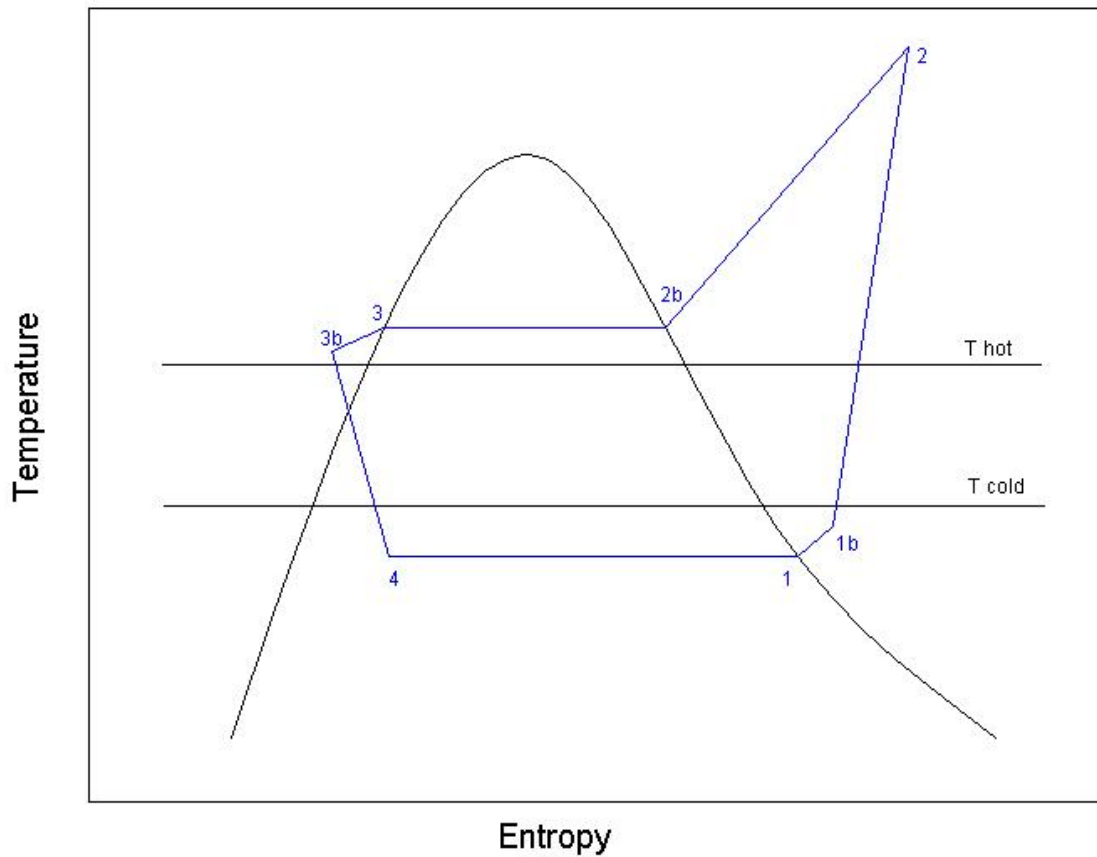


Figure B.4. Modified Rankine Cycle

The chiller capacity may increase depending on whether the superheating of the vapor occurs in the evaporator or in the pipe connecting the evaporator and compressor. If an increase in capacity due to superheating is realized, it should be very small in comparison with the capacity due to evaporation. For practical purposes, the capacity will still be the area under the evaporation line (4-1). The work now becomes the area under the line 2-3b minus the capacity. The relationship between capacity and work is shown in Figure B.5.

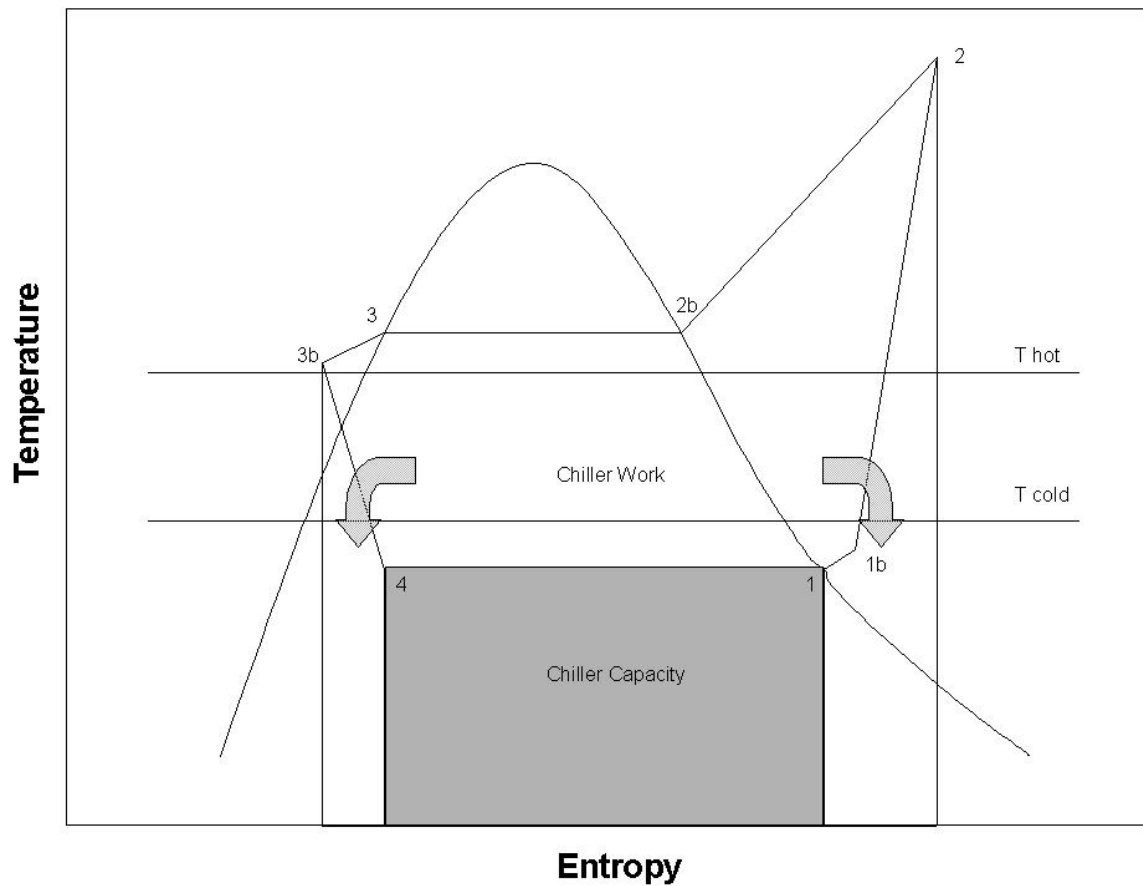


Figure B.5. Rankine Cycle with capacity emphasized

Figure B.5 may also be used to show the work associated with individual stages in the cycle. For instance, the area under the line 1b-2 is the amount of work done to overcome compressor irreversibilities. The area under the line 1-1b is the work associated with the superheating of the refrigerant vapor. By using the temperature-entropy diagram, each component that contributes to the work required to achieve the capacity may be investigated. The breakdown of these individual components is shown

in Figure B.6 below. Figure B.6 shows how the T-s diagram effectively demonstrates the losses associated with each chiller component.

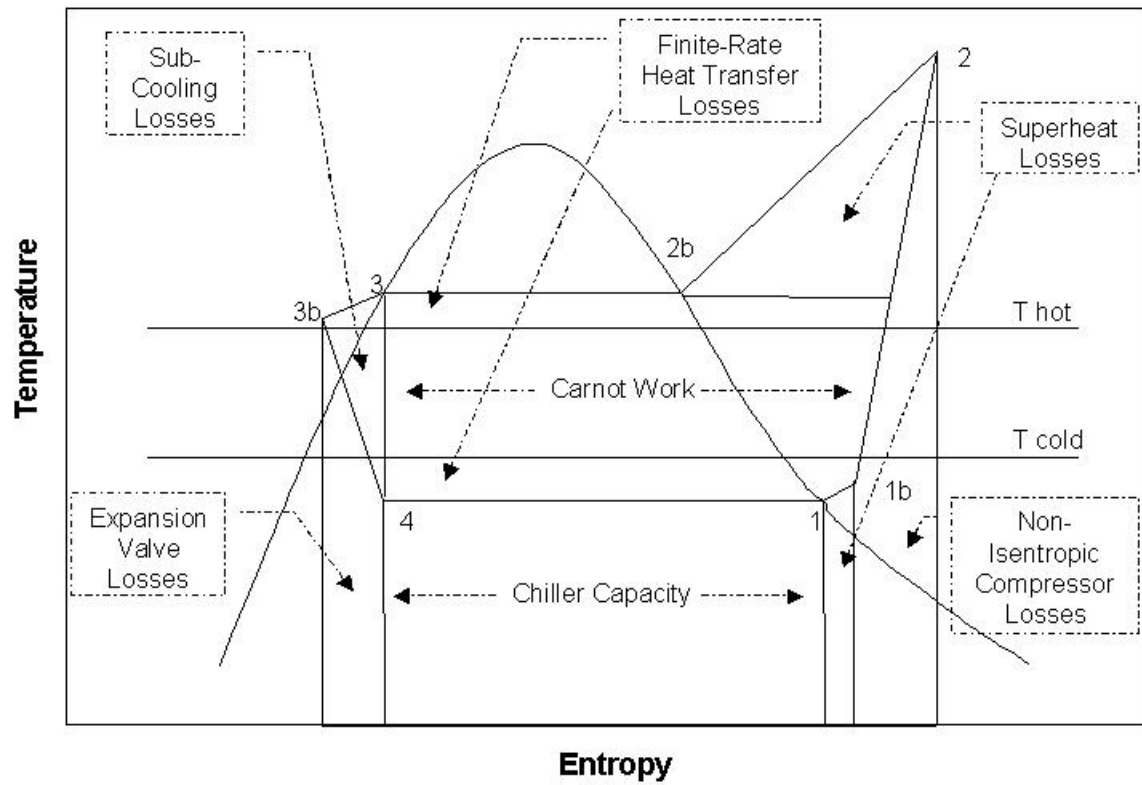


Figure B.6. Rankine Cycle with irreversibilities



## VITA

### **Rhett David Graves**

Project Analyst, Energy Solutions

TAC Americas

Carrollton, TX 75006

#### **Personal Data**

**Birth Date and Place:**

September 03, 1977, Sweetwater, TN

**Home Address:**

342 White Road West  
Collierville, TN 38017

**Marital Status:**

Single

#### **Education**

Master of Science, Mechanical Engineering, Texas A&M University,  
College Station. December 2003.

Bachelor of Science, Mechanical Engineering, Mississippi State University,  
Mississippi State. May 2001.